Wildfire smoke exposure and mortality burden in the US under future climate change

Minghao Qiu [1,2,*], Jessica Li [3], Carlos F. Gould [4], Renzhi Jing [2,5,6] , Makoto Kelp [1], Marissa L. Childs [7], Jeff Wen [1], Yuanyu Xie [8], Meiyun Lin [9], Mathew V. Kiang [10], Sam Heft-Neal [3], Noah S. Diffenbaugh [1], Marshall Burke [1,3,11]

1 Doerr School of Sustainability, Stanford University, Stanford, CA, USA

2 Center for Innovation in Global Health, Stanford University, Stanford, CA, USA

3 Center on Food Security and the Environment, Stanford University, Stanford, CA, USA

4 School of Public Health, University of California San Diego, La Jolla, CA, USA

5 Woods Institute for the Environment, Stanford University, Stanford, CA, USA

6 Department of Medicine, School of Medicine, Stanford University, Stanford, CA, USA

7 Center for the Environment, Harvard University, Cambridge, MA, USA

8 School of Public Policy and International Affairs, Princeton University, Princeton, NJ, USA

9 National Oceanic and Atmospheric Administration Geophysical Fluid Dynamics Laboratory, National Oceanic and Atmospheric Administration, Princeton, NJ, USA

10 Department of Epidemiology and Population Health, School of Medicine, Stanford University, Stanford, CA, USA

11 National Bureau of Economic Research, Cambridge MA, USA

***** To whom correspondence should be addressed. E-mail: mhqiu@stanford.edu

The paper is a non-peer reviewed preprint submitted to EarthArXiv. It has also been submitted for publication in a peer reviewed journal, but has yet to be formally accepted for publication. If accepted, the final version of this manuscript will be available via the "Peer-reviewed Publication DOI" link on the EarthArXiv page for this paper.

Abstract

Wildfire activity has increased in the US and is projected to accelerate under future climate change. However, our understanding of the impacts of climate change on wildfire smoke and health remains highly uncertain. Here we quantify the mortality burden in the US due to wildfire smoke fine particulate matter ($PM_{2.5}$) under future climate change. We construct an ensemble of statistical and machine learning models that link climate to wildfire smoke $PM_{2.5}$, and empirically estimate smoke $PM_{2.5}$-mortality relationships using georeferenced data on all recorded deaths in the US from 2006 to 2019. We project that climate-driven increases in future smoke $PM_{2.5}$ could result in 27,800 excess deaths (95% confidence interval: 13,100 - 43,400) per year by 2050 under a high warming scenario (SSP3-7.0) – a 76% increase relative to estimated 2011-2020 averages. Cumulative excess deaths from wildfire smoke $PM_{2.5}$ could exceed 700,000 between 2025-2055. When monetized, climate-induced smoke deaths result in annual damages of $244 billion, comparable to prior *aggregate* estimates of all other economic damage due to climate change. Our research suggests that the health cost of climate-driven wildfire smoke could be among the most important and costly consequences of a warming climate in the US, and an urgent adaptation priority.

Introduction

Wildfire activity has increased substantially over the US in the last two decades, with the largest increases observed in the western US (*1–5*). As a result, air pollution that is associated with wildfire smoke (specifically fine particulate matter, $PM_{2.5}$) has significantly increased (*6–9*). Given established relationships between ambient smoke $PM_{2.5}$ exposure and poor health (*10–13*), these increases have likely worsened several health outcomes. In many parts of the western US, smoke $PM_{2.5}$ accounted for over 50% of the annual concentration of $PM_{2.5}$ in extreme smoke years (*14*, *15*), and has led to stagnation or even reversal of the otherwise declining trend in ambient $PM_{2.5}$ over the last two decades due to the Clean Air Act (*16*).

Mounting evidence has suggested that human-induced climate change is a leading cause for the increased wildfire activity, especially in forested areas in the western US (*2–4*, *17–19*), alongside other important causes that include historical fire suppression and the expansion of human activities into forested areas (*20*). A warming climate can influence wildfire activities by altering the aridity of the fuel (*2*, *21*), conditions for fire spread (*22*, *23*), as well as lightning ignitions (*24*). For the western US, many studies have projected increasing wildfire risks under a warming climate primarily due to increasing fuel aridity under higher ambient temperature (*25–27*).

However, the relationship between a warming climate and the resulting increase in wildfire smoke and health impacts is not fully understood and highly uncertain. Several studies use regression models or land-vegetation-fire models to first project the wildfire activities under future climate and then utilize chemical transport models to estimate changes in smoke $PM_{2.5}$ concentrations (*28–32*) and associated health outcomes (*33–36*). However, prior projections of future mortality due to climate-driven fire smoke span a wide range of uncertainties (*37*) – reflecting an important knowledge gap given the large potential impacts. Uncertainties in the prior projections come from three key sources. First, large uncertainties exist in how wildfire emissions respond to climate change (*38*). Second, modeling fire impacts on surface $PM_{2.5}$ often faces large uncertainty in emission inventories (*39*, *40*), the vertical distribution of emission profiles (*41*), and fire-weather interactions (*42*), which results in modeled smoke concentration sometimes differ by an order of magnitude when compared to surface observations (*43*). Third, most prior studies quantify the health impacts of smoke $PM_{2.5}$ by applying existing concentration-response functions derived from total $PM_{2.5}$ exposures, which could fail to capture unique health impacts of smoke $PM_{2.5}$ exposure, such as from smoke-specific chemical composition and toxicity (*44*) or behavioral responses unique to smoke events (*13*).

Because of these challenges, very few studies to date have projected future smoke $PM_{2.5}$ concentrations using empirically grounded relationships between climate, wildfire, and $PM_{2.5}$ (*35*, *45*). To our knowledge, no studies have estimated the future smoke mortality burden accounting for the unique health impacts of smoke $PM_{2.5}$ using dose-response functions that are specific to smoke pollution exposure. Absent this quantification, leading estimates of the societal impact of climate change – many of which are directly used to guide policy – do not incorporate potential mortality impacts due to wildfire smoke $PM_{2.5}$ (*46–48*). Detailed projections of future smoke $PM_{2.5}$ exposure and health burden are crucial to inform policies to mitigate and adapt to the negative impacts of smoke $PM_{2.5}$ on humans.

In this paper, we develop a comprehensive, data-driven approach that directly address all three of the above challenges. First, to improve understanding of the climate-fire emissions relationship, we construct an ensemble of statistical and machine learning models that predict fire emissions as a function of climate and land-use variables over North America (including Mexico and Canada), using observational data from 2001-2021. By using historical data that includes recent years with extreme weather conditions (e.g., drought in the western US in 2020), which is projected to increase under future climate change, our ensemble of models can better characterize how climate influences wildfire emissions in future scenarios. We use dry matter emissions from the fourth version of the Global Fire Emissions Database with small fires (GFED4s) (*49*), which include fire emissions from agriculture fires and land-use change. However, as wildfire emissions dominate in most of our studied regions (especially in the western US and Canada where we see the largest effects, see Table S1), we refer to our estimates as "wildfire emissions" and "wildfire smoke $PM_{2.5}$" for simplicity and consistency. By modeling changes in wildfire emissions in Canada and Mexico, our approach can also capture important transboundary influences on US smoke $PM_{2.5}$ and health effects, such as those that occurred in the summer of 2023 (*50*). Second, we use surface wildfire smoke $PM_{2.5}$ estimates from (*8*) to establish an empirical relationship between wildfire emissions and smoke $PM_{2.5}$ concentration across the contiguous US at 10 km resolution, accounting for variation in wind directions and spatial transport. Our approach fits the observed surface $PM_{2.5}$ data well (Figure S2), and allows us to efficiently predict smoke concentration in one location from changes in wildfire emissions in another (Methods). Third, to address the challenge of accurately estimating the health impacts of ambient smoke exposure, we empirically estimate the effects of annual smoke $PM_{2.5}$ concentration on annual mortality rates using county-level data from 2006 to 2019 on all recorded deaths in the US. We estimate dose-response functions using a Poisson model in which we allow non-linear impacts of smoke $PM_{2.5}$ on mortality rates, consistent with prior papers that examine smoke impacts on mortality and other health outcomes (*13*, *51*), while flexibly controlling for temperature, precipitation, and a broad range of possible spatial and temporal confounds (Methods).

Finally, we combine the empirical relationships between climate, wildfire emissions, smoke $PM_{2.5}$, and mortality rates derived above with projected climate variables derived from CMIP6 global climate model ensembles to generate future projections of smoke $PM_{2.5}$ and mortality burden. We project the annual average smoke $PM_{2.5}$ concentration in each 10 km location across the contiguous US (48 states and the District of Columbia) between 2046 and 2055 under different climate scenarios. We then quantify changes in mortality rates in each county in the contiguous US between 2050 and the historical period, and the difference across three climate scenarios (SSP1-2.6, SSP2-4.5, and

SSP3-7.0) to quantify the potential health benefits from climate mitigation and adaptation. We quantify the uncertainty in the final projected mortality burden across the different components of our modeling framework and compare our mortality estimates with estimates of direct temperature-related mortality burden and aggregate climate costs from prior work (*46*, *52*, *53*) to contextualize the importance of climate-smoke channels relative to other known climate impacts.

Results

Empirical relationship between climate and smoke $PM_{2.5}$

We considered three different statistical and machine learning frameworks for modeling the climate-fire relationship (Methods). To account for geographical heterogeneity, we estimated each of our frameworks separately by region, resulting in five ensembles of climate-fire models. Our models can capture the variability of wildfire dry matter emissions at 10-year intervals (to account for fire stochasticity at the annual level, see Methods), highlighting their ability to quantify changes in wildfire emissions under different climate conditions (Figure 1A). When evaluating through cross-validation of temporal blocks (i.e. randomly splitting a time series of observations into disjoint sets of training and testing years), our models achieve high prediction performance, especially in the western US, Canada, and Mexico, with correlation coefficients of 0.87-0.95 in the out-of-sample evaluations (Table S2). Under these evaluation criteria, our model achieves higher performance relative to other commonly-used regression methods such as a log-linear model to model climate impacts on burned area (*2*), as well as more flexible machine learning methods (*38*) (Figure S1). However, the model performance indicates that climate conditions are not the only factors influencing the variability of wildfire emissions over time. For example, we find that the model performs less well in the southeastern US and northeastern US, where many fires are agricultural or prescribed fires, which are less directly influenced by climate factors (*54*). Furthermore, while our models can predict spatially- and temporally-aggregated emissions effectively, the predictive performance deteriorates when the same model is evaluated at finer temporal and spatial resolutions (Figures S3 and S4). Such evaluation results are consistent with prior literature on global fire modeling (*55*). Our findings suggest that, although climate conditions such as low soil moisture and high ambient temperatures are related to enhanced fire activity in aggregate, whether a fire occurs in a specific location depends on more stochastic factors such as lightning and human ignitions that are very hard to predict (*56*).

Combining our statistical and machine learning models with future climate projections from CMIP6 global climate models, we project that wildfire emissions will increase by 2050 in all study regions except for the eastern US (Figure 1B). The largest increases in wildfire emissions are projected in the western US, where the model estimates that the annual wildfire emissions will increase by between 248% (SSP1-2.6) and 470% (SSP3-7.0) in the 2050s relative to average emissions during

2011-2020. When compared to 2020, the largest wildfire year for the western US in our historical data, projected annual wildfire emissions during the 2050s will either reach (as in the case of SSP1-2.6) or exceed (by 34% under SSP2-4.5 or 62% under SSP3-7.0) emissions observed in 2020. This magnitude of increases is largely consistent with prior estimates of the western US derived from statistical models and process-based models (*26*, *27*, *31*). Consistent with prior literature, we find that decreased soil moisture and increased ambient temperature, especially in the forest areas in the western US, are the leading contributors to increased wildfire emissions (Figure S5, Table S3, Table S4). In the eastern US, we estimate a decrease of wildfire emissions by 15% under SSP1-2.6 and an increase of wildfire emissions by 10% under SSP3-7.0. These opposing predictions are driven by a combination of two conflicting factors: projected increases in ambient temperature, which increase emissions, and projected increases in precipitation, which decrease projected emissions (Figure S5). Our projected patterns in the eastern US are consistent with a prior study that used a process-based fire-climate model (*31*). By the 2050s, we project an increase in emissions of 33-43% in Mexico, and of 30-49% in Canada, relative to average emissions during 2011-2020, in large part due to projected increases in Vapor Pressure Deficit (VPD).

To link wildfire emissions to smoke $PM_{2.5}$ concentrations, we develop an empirical relationship that accounts for wind direction, distance from fire, and geographical region (Figure 2). As shown in Figure 2A, we find that wildfire emissions increase smoke $PM_{2.5}$ concentrations near an active fire, with the effects gradually decaying as the distance from the fire increases. Consistent with previous evidence of long-range transport of smoke (*57*, *58*), we find a statistically significant effect ($p<0.05$) of wildfire emissions on downwind locations up to 1000 km away. We find substantial regional heterogeneity in the impacts of dry matter emissions on wildfire $PM_{2.5}$ (Figure 2B). For example, we find that one ton of dry matter emissions (as estimated in GFED4s fire emissions database) can generate as much as 3x surface smoke $PM_{2.5}$ in the Northwest compared to the Southwest and South. Such regional heterogeneity likely reflects a multitude of factors, such as vegetation type, vegetation density, and fire intensity (Methods).

Projected smoke $PM_{2.5}$ concentration under future climate

As a result of projected rising wildfire emissions, we find increases in annual smoke $PM_{2.5}$ concentrations throughout the US in 2050 under all future climate scenarios (Figure 3A). Under our highest warming scenario (SSP3-7.0), we estimate that annual average smoke $PM_{2.5}$ concentration could reach 10 $\mu g/m^3$ in some regions on the west coast, a level that has only been observed in extreme smoke years such as 2020 (*8*). While the most substantial changes in smoke $PM_{2.5}$ happen across the western US, smoke $PM_{2.5}$ concentrations are also projected to increase in the northeast US, largely due to projected increases in wildfire emissions in the western US and Canada and subsequent increases in cross-boundary transport of wildfire smoke from these fires.

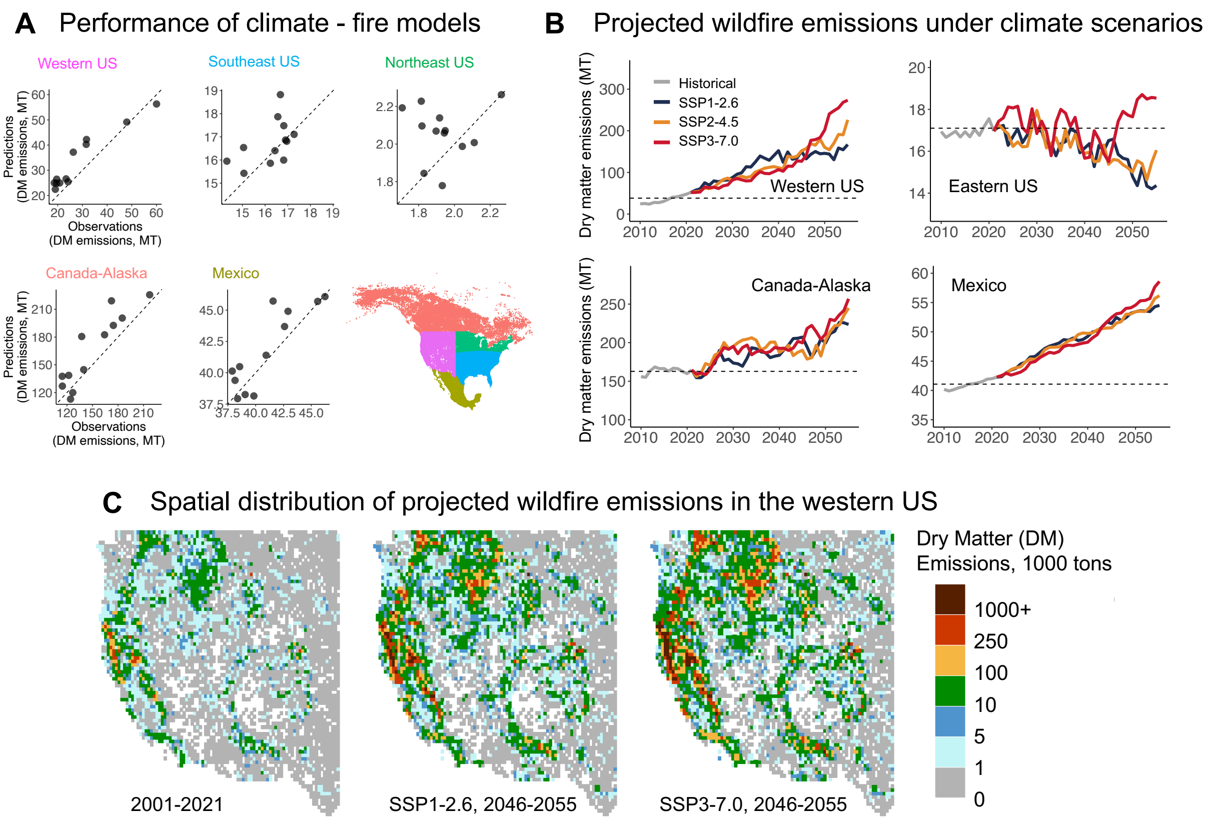

Figure 1: **Projected wildfire emissions under future climate change scenarios.** Panel A: Performance of the statistical and machine learning ensemble models. We build separate models to predict wildfire Dry Matter (DM) emissions for five regions respectively: Western US, Southeast US, Northeast US, Canada-Alaska, and Mexico. The plot shows the 10-year moving average of predicted emissions (y-axis) against the observed emissions (x-axis), aggregated at the regional level. Panel B: Projected wildfire emissions (unit: Million Tons, MT) under the historical scenarios and three future climate scenarios (SSP1-2.6, SSP2-4.5, and SSP3-7.0). The plot shows the 10-year moving average of the wildfire emission projections. The dashed line represents the average observed emissions over 2001-2021 for each region. For presentation purpose, we aggregate predictions from northeast US and southeast US to calculate the total for eastern US. Panel C: Observed DM emissions at the native resolution (0.25 degree) in 2001-2021 from GFED4s, and projected annual emissions averaged between 2046-2055 under SSP1-2.6 and SSP3-7.0 scenarios (down-scaled from aggregated projections).

We find that the relative contribution of wildfire smoke to total population-weighted $PM_{2.5}$ increases by 240-320% in 2050. This finding holds even if non-smoke $PM_{2.5}$ remains constant – a conservative assumption given recent and ongoing declines in non-smoke $PM_{2.5}$ concentrations (*16*). We estimate that smoke $PM_{2.5}$ will account for 13-17% of total population-weighted $PM_{2.5}$ in the US in 2050, which is 2-3x its contribution of 5.4% during 2011-2020. Wildfire smoke will account

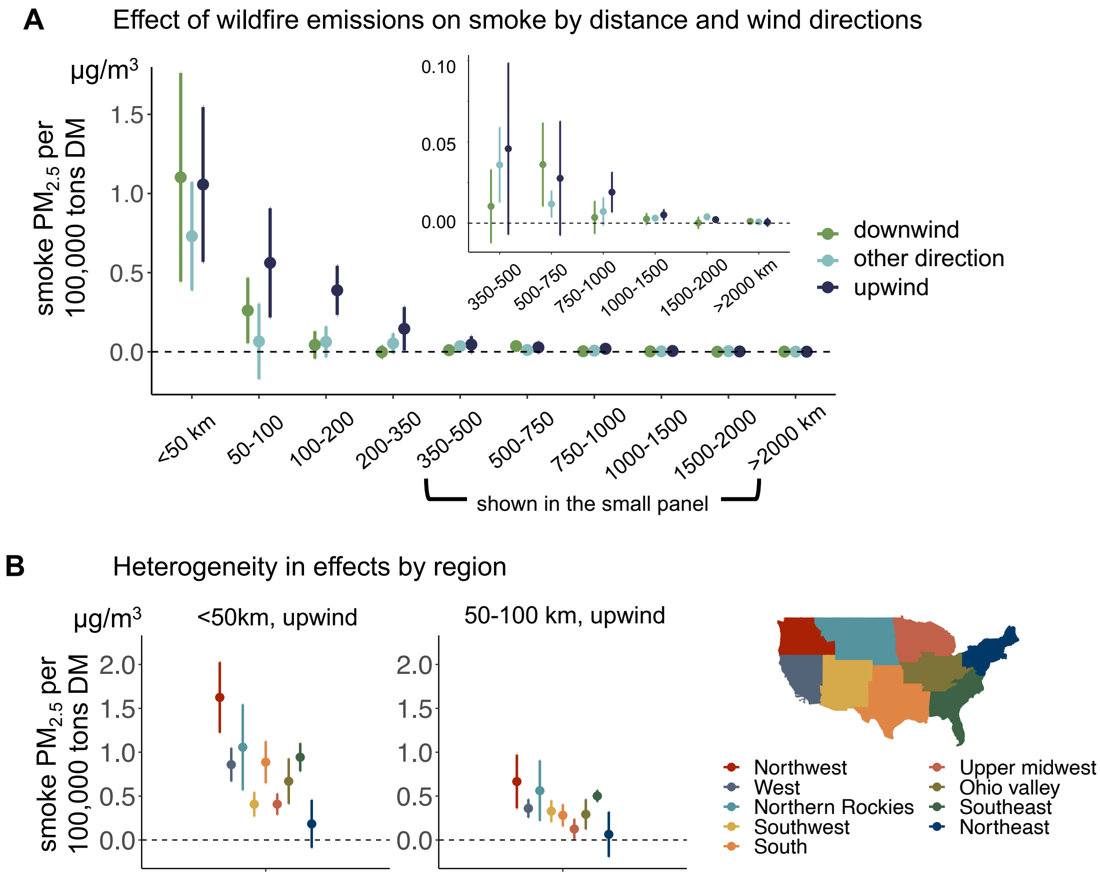

Figure 2: **Wildfire emissions increase the observed smoke $PM_{2.5}$ concentration in the neighboring and downwind areas.** Panel A: The empirically estimated effects of wildfire emissions on smoke $PM_{2.5}$ by distance from emissions and wind directions. "Upwind" means the fire is upwind of the location at which $PM_{2.5}$ is measured. Wildfire emissions are estimated to have larger impacts on smoke $PM_{2.5}$ when smoke location is closer to fire (distance to emissions is shown on the x-axis), and when wildfire emissions happen upwind of the smoke locations (wind patterns shown in colors). Separate models are estimated for the 9 climatic regions in the US determined by National Centers for Environmental Information (as shown in Panel B). Panel A shows the results in the *Northern Rockies* region. Panel B: Regional heterogeneity in emission impacts on smoke $PM_{2.5}$. Panel B shows the estimated effects of *upwind* emissions in the <50 km and 500-100 km bins, across the nine regions in the US.

for at least 15% of total population-weighted $PM_{2.5}$ in 17 states, including states both in the West such as Oregon (with 61% smoke contribution), Washington (56%), and California (30%), as well as states in the South and Midwest such as Oklahoma (19%) and Minnesota (16%). Figure 3B shows the smoke contribution in the top 10 states (see Table S5 for more states).

Under the SSP3-7.0 scenario, average population-weighted smoke $PM_{2.5}$ exposure is projected to reach 1.47 $\mu g/m^3$, an increase of over 200% relative to the average level between 2011-2020 (Figure

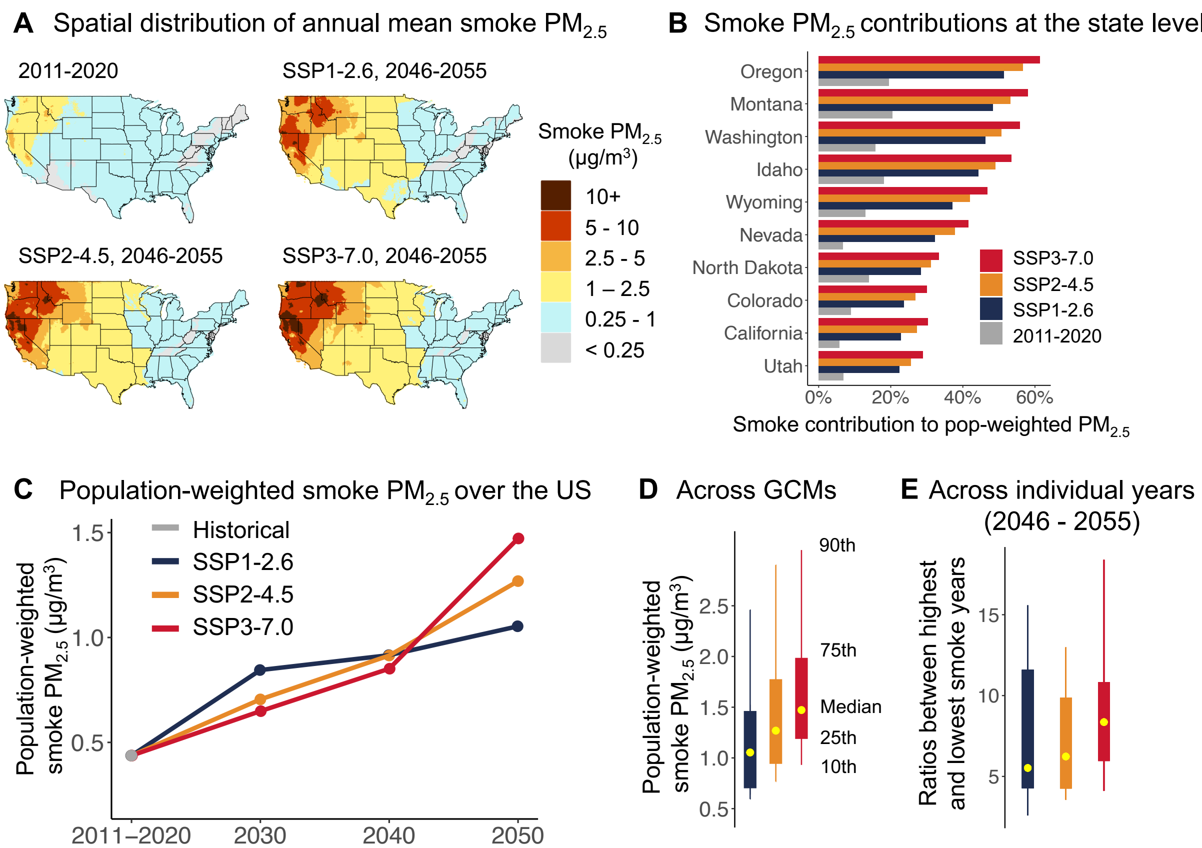

Figure 3: **Population exposure to wildfire smoke $PM_{2.5}$ increases by 2- to 3-fold under future climate change scenarios.** Panel A: The annual mean smoke $PM_{2.5}$ concentration in the historical data (2011-2020), and projected annual mean smoke $PM_{2.5}$ concentration under the three climate scenarios in 2046-2055. Panel B: the contribution of smoke $PM_{2.5}$ to total population-weighted $PM_{2.5}$ at the state level. Non-smoke $PM_{2.5}$ is calculated as the difference between total $PM_{2.5}$ (derived from (*59*)) and smoke $PM_{2.5}$ in 2016-2020, and is assumed to be constant in future. The panel only lists the top ten states with the highest smoke contribution under SSP3-7.0 scenario in 2050. Panel C: population-weighted smoke $PM_{2.5}$ over the US in different decades. Panel D: uncertainty in the population-weighted smoke $PM_{2.5}$ across the 28 GCMs used in the projection. Panel E: for each GCM, we calculate the ratio between the highest and lowest projected population-weighted smoke $PM_{2.5}$ during 2046-2055. The panel shows the quantiles of these ratios across the 28 GCMs.

3C), and 1.6x the population-weighted smoke $PM_{2.5}$ concentration in the historically extreme year of 2020 (0.90 μg/m^3). The differences across the three climate scenarios are negligible in 2030 and 2040 due to little difference in projections of the climate variables (Figure S5). However, by the 2050s, population-weighted smoke $PM_{2.5}$ is meaningfully smaller in the low warming scenarios, at 1.05 μg/m^3 under SSP1-2.6 or 1.27 μg/m^3 under SSP2-4.5, averaged across GCMs. Some individual

GCMs project much larger or smaller increases (Figure 3D). Also, these estimates represent decadal averages of annual smoke $PM_{2.5}$ concentrations, in this case averaged 2046 to 2055. Given interannual climate variability, projections suggest that average smoke $PM_{2.5}$ concentrations in individual years could differ substantially, with the highest projected smoke year having roughly 5-10x the concentration of the lowest year (Figure 3E). Our method likely underestimates the interannual variability as it does not capture variability in non-climate factors.

Mortality burden due to smoke $PM_{2.5}$ exposure

We find that exposure to annual smoke $PM_{2.5}$ increases all-age mortality rates (Figure 4A), even at low smoke concentrations (<1 μg/m^3), consistent with recent evidence from studies of low levels of all-source $PM_{2.5}$ (*60*). Compared to a year of zero or minimal smoke $PM_{2.5}$ (annual mean concentration <0.1 μg/m^3), we find that a year with annual average smoke $PM_{2.5}$ of 0.75-1 μg/m^3 increases county-level mortality rate by 1.3% (95%CI: 0.6%, 2.0%). Years with extreme ambient wildfire smoke concentrations (>6 μg/m^3) increase annual mortality rates by 5.8% (95%CI: 2.2%, 8.9%). Wildfire smoke increases mortality rates among both the elderly and the general population (Figure S6). Our estimated smoke-mortality relationship is similar in shape to the results estimated by (*51*) at the county-month level. For a given increase in $PM_{2.5}$ concentration by 1 μg/m^3, our observed effects for smoke $PM_{2.5}$ exceed a recent meta-analysis estimate for all-source $PM_{2.5}$ (0.8% increase in mortality rates per 1 μg/m^3 (*61*)), although our confidence interval contains this lower estimate.

Combining our empirically-derived dose-response function and historical smoke $PM_{2.5}$ concentrations, we estimate that smoke $PM_{2.5}$ caused 15,800 excess deaths (95% CI: 6900, 25300) per year during 2011-2020 (Figure 4B), relative to a counterfactual of no smoke $PM_{2.5}$. This number of smoke-related deaths would account for 9.2% of total estimated deaths due to total (smoke and non-smoke) $PM_{2.5}$ exposure during the same period (estimated using the response function from (*61*) and total $PM_{2.5}$ estimates from (*59*)). As shown in Figures 4B and S7, roughly 90% of estimated excess deaths from wildfire smoke exposure come from relatively low but frequent exposures to annual concentrations below 1 μg/m^3.

We estimate that smoke $PM_{2.5}$ will cause 23,800 to 27,800 annual excess deaths by mid-century across the three climate scenarios – an increase of 51-76% in mortality burden from smoke relative to 2011-2020. Even under the low warming scenario (SSP1-2.6), we estimate that smoke $PM_{2.5}$ will lead to 8,000 more annual excess deaths in the 2050s relative to today. Over the period of 2025-2055, we estimate that wildfire smoke$PM_{2.5}$ could lead to cumulative excess deaths of 690,000 (SSP1-2.6) to 720,000 (SSP3-7.0). Although in the historical period, annual mean wildfire smoke concentrations above 5 μg/m^3 were rare and represented only 3% of the total mortality burden (Figure 4A), we estimate that these more extreme years will account for between 20-26% of the total excess deaths from smoke in the 2050s (Figure S7). The climate-induced smoke deaths are distributed across populous counties in the western US as well as in the Midwest, Northeast, and South (Figure 4C). The top five states that are predicted to experience the largest increases in annual smoke $PM_{2.5}$ deaths in 2050s under SSP3-7.0 are California (3300 excess deaths per year), Washington (900), Texas (680), Oregon (610), and Florida (380). While projected smoke concentrations are highest in the western US, almost half of the smoke mortality come from eastern states (east of 95° W) due to higher population densities and damages from low wildfire smoke concentrations (Figure S8 and Table S7). Estimated mortality effects are largely robust across alternative specifications of the smoke-mortality models including alternative functional forms, temporal aggregations, and bin definitions (Figure S9 and S10).

We contextualize the magnitude of these mortality impacts in two ways. First, we compare our estimates of excess deaths from climate-driven smoke $PM_{2.5}$ to the direct effects of extreme temperatures on mortality – an impact which has been the primary focus of climate change impacts on mortality and is projected to be one of the leading economic costs of global climate change (*47*, *48*, *52*, *62*). Recent studies find that, by mid-century in the US, increasing mortality from more frequent extreme heat is likely to be more than offset by declining mortality due to cold weather with a projected decrease in annual excess deaths of 15,800 by mid-century (under the SSP2-4.5 scenario) compared to 2001-2010 (*52*). Our projected increase in smoke mortality over the same period represents 62% of this reduction in direct temperature-related deaths (Figure 4D), significantly offsetting a potential benefit of future warming in the US. However, as shown in Figure 4E, the size of this offset differs across the US, with certain states likely to suffer compounded consequences from increases in both smoke-related and heat-related deaths (e.g., CA, TX, FL), and other states likely to see minimal smoke-related mortality and a substantial decline in heat-related deaths (e.g., IL).

As a second comparison, we compare our estimates of climate-induced smoke damages with two prior estimates of aggregated monetized damage due to climate change. Using a Value of Statistical Life (VSL) of $10.95 million dollars (year 2019 dollars, as suggested by EPA (*63*)), we find that the projected 12k increase in annual excess deaths due to climate-driven wildfire smoke would result in annual damages of $244 billion in 2050 (not discounted, in year 2019 dollars, see Methods). Under a similar projected warming level of SSP3-7.0 scenario, Hsiang et al. (*46*) estimated annual damage of 0.4%-0.8% of US GDP or $166-332 billion (in year 2019 dollars, using annual projected GDP of $38.5 trillion from (*53*)), which included damages from temperature-related mortality, agriculture, crime, coastal storms, energy, and labor channels. The Framework for Evaluating Damages and Impacts (FrEDI), developed by US EPA (*53*), considered more sectors (including estimated wildfire damages from the western US (*35*)) and estimated annual damage of $292 billion in 2050s. Our estimates suggest that damages from increase smoke-related mortality could roughly equal damages from all other estimated causes by mid-century in the US.

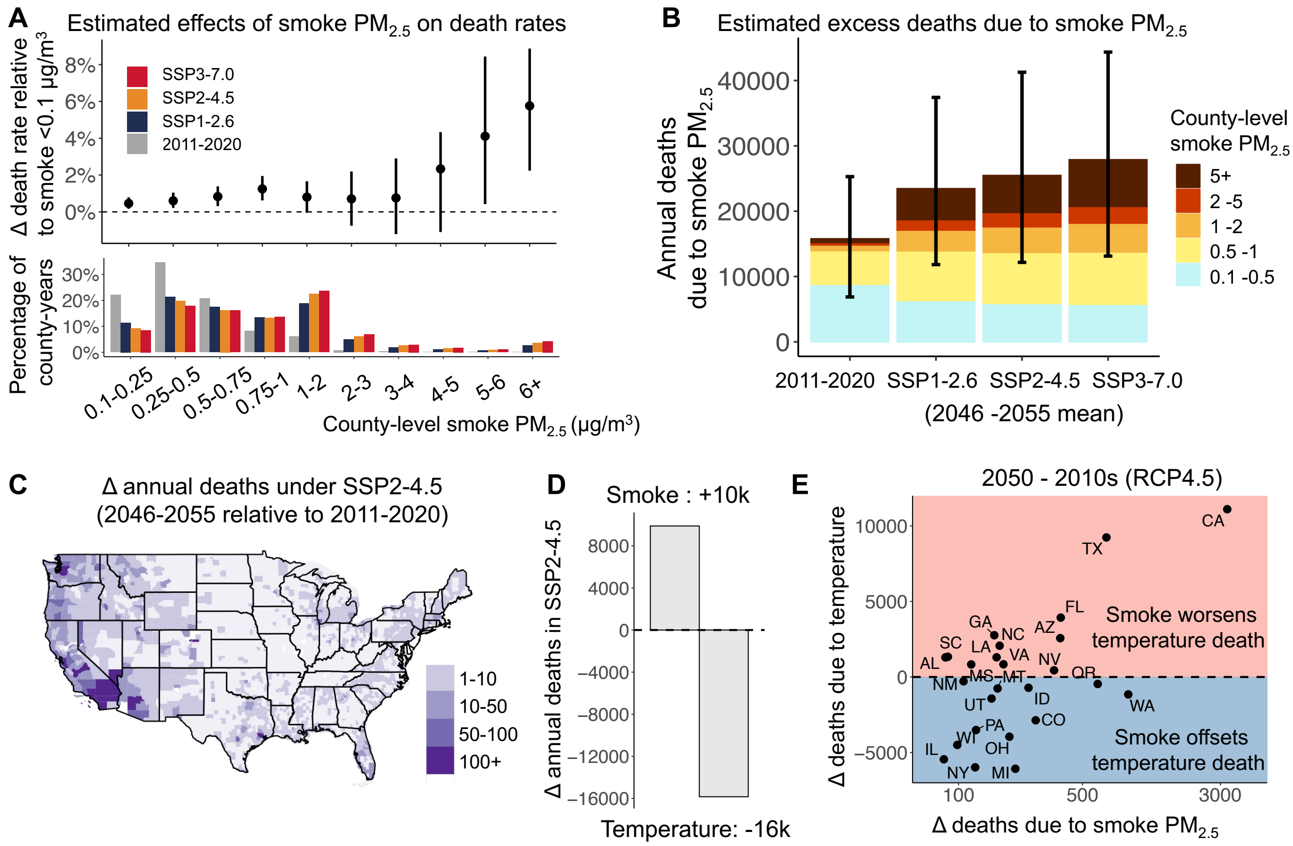

Figure 4: **Mortality impacts of wildfire smoke $PM_{2.5}$ and estimated mortality due to smoke $PM_{2.5}$ under future climate scenarios.** Panel A: empirically estimated effects of annual smoke $PM_{2.5}$ concentration on county-level all-age annual mortality rates. The figure shows the effects of exposure to different annual mean concentration of smoke $PM_{2.5}$ (shown in the x-axis) relative to a year with smoke concentration <0.1 $\mu g/m^3$, estimated using a Poisson model at the county and annual level and data from 2006-2019. The error bars show the 95% confidence interval estimated using bootstrap. The bottom part of panel A shows the percentage of county-years in each smoke concentration bin over the historical period (2011-2020) as well as future climate scenarios (2046-2055). Panel B: estimated annual excess deaths due to smoke $PM_{2.5}$, and contribution to total smoke excess deaths from different smoke concentration bins. The error bars show the 95% bootstrapped confidence intervals. Panel C: county-level projected increases in annual excess deaths due to smoke $PM_{2.5}$ in 2050; increases are calculated as the differences between the average deaths under SSP2-4.5 scenario over 2046-2055 and the 2011-2020 average. Panel D shows US-wide total estimated annual smoke deaths and direct temperature-related deaths in 2050, with increasing smoke deaths offsetting 62% of the reduction in temperature deaths. Panel E: projected increase in smoke deaths offsets projected reductions in direct temperature-related deaths by 2050s, the latter as estimated in a recent study (*52*). The x-axis shows the changes in deaths due to smoke $PM_{2.5}$ in 2050s (note the log-scale), and the y-axis shows the changes in deaths due to temperature change, where only the 25 states with >75 smoke related deaths per year are visualized.

Discussion

While the effects of climate change on wildfire smoke and human health have become an emerging research topic, these effects are rarely incorporated into estimates of climate impacts. In this study, we estimate that climate-induced smoke $PM_{2.5}$ could lead to 12k additional excess deaths per year under the SSP3-7.0 scenario in the US, substantially offsetting the reduction in direct temperature-related deaths expected due to climate change. These estimated deaths lead to an amount of monetized damage on par with quantified damages from all other sectors combined. Our results suggest that increasing wildfire smoke pollution due to climate change could be one of the most important and costly consequences of a warming climate in the US.

We find that aggressive mitigation of global greenhouse gas emissions would limit increases in smoke-related deaths, but that such deaths are likely to increase substantially even under low-emission scenarios. This finding points to the urgent need for future adaptation if damages are to be avoided. Adaptation could occur at many points along the wildfire-smoke-mortality chain. Increased fuel management, such as prescribed burning, could reduce the likelihood of extreme wildfire activity during adverse climate conditions, but will create smoke of its own; while the reduction in smoke from high-intensity fire is likely to substantially outweigh the increase from purposeful low-intensity fire, quantifying such tradeoffs is another critical area for work (*64–66*). Adaptation could also target the relationship between smoke and adverse health outcomes. This could include better informing individuals of, and protecting them from, smoke that does occur as current reliance on individuals to self-protect appears highly inadequate and inequitable (*67*, *68*). Improved indoor filtration, including low-cost portable filters, appears a particularly promising and scalable solution, and ensuring that such filtration is affordable, accessible, and used is a potential policy priority (*69*).

Using georeferenced data on deaths and ambient wildfire smoke concentrations, we show that increasing annual exposures to smoke $PM_{2.5}$ are associated with higher county-level annual mortality rates across the contiguous US. Our work contributes to a large literature documenting the impacts of annual exposures to total $PM_{2.5}$ on mortality, which has shaped decades of policy to improve ambient air quality in the US. Due to our annual level projections of wildfire smoke, impacts of wildfire smoke on mortality were necessarily conducted at the annual level. However, wildfires are episodic and typically generate short-term spikes in ambient air pollution, which our measure of exposure may partly obscure (*70*). As such, our results are a complement to other studies on the health effects of short-term (e.g., daily) wildfire smoke exposures (*12*).

We find that elevated long-term average smoke $PM_{2.5}$ concentrations increase mortality rates at both low and high concentrations. These increases lead to two important implications. First, we project large mortality burden not only in regions where large fires occur but also in populous regions with low smoke concentrations (e.g., the eastern US) that have historically received less focus in wildfire studies. We find that 67% of the estimated historical smoke mortality and 42% of the projected future mortality come from the eastern US, as a result of increases in low-level smoke concentrations, consistent with previous historical estimates from (*57*). Second, despite larger differences in projected smoke $PM_{2.5}$ concentration across the three climate scenarios, we estimate substantial mortality increases even in the low warming scenario (SSP1-2.6), again because this scenario generates low-level annual concentration increases that we estimate can have substantial mortality impacts. Our projected mortality impacts are in the uncertainty band of one prior study that applied a range of dose-response functions of total $PM_{2.5}$ exposure (*34*), while substantially higher than the other estimate which only focuses on the western US (*35*), in part due to the mortality impacts we find at low exposure levels.

Our approach can isolate the "direct" impacts of climate change on wildfire air pollution, but does not account for potential "indirect" effects of climate on wildfire through channels such as climate's influence on vegetation growth or lightning-related ignitions. Existing evidence has suggested that vegetation overall would increase under higher warming levels, which could lead to higher wildfire emissions and smoke (*27*). Furthermore, we did not attempt to model the many non-climate factors that contribute to wildfire activity, including the location of energy infrastructure, distance to road, housing development, and fire suppression efforts. Instead, we sought a model that could isolate the influence of climate while holding these other factors fixed. If these factors change dramatically in the future, then our estimates could understate or overstate future emissions, smoke, and mortality. For example, if expansions of houses near wildland vegetation continue (*20*), the effects of a warming climate on wildfire emissions could be larger given more human ignitions, particularly as population growth in the wildland-urban interface has been most rapid in areas where the vegetation is most vulnerable to wildfire (*71*). Alternatively, large increases in wildfire activity could be self-limiting as fires regulate the amount and availability of fuel load for future combustion. Existing studies suggest that this feedback is likely modest (*26*), but constraining this feedback empirically is a critical area for future work.

Our projection analysis quantifies the key uncertainties in climate-wildfire-smoke-mortality estimations (Figure S11). Addressing these uncertainties could further improve understanding of the climate influences on wildfire pollution and health, and thus inform relevant policies. One of the largest uncertainties is how climate change will influence wildfire emissions and smoke $PM_{2.5}$. The statistical models we train can predict the emissions well given observational data, but we know little about their ability to predict wildfire levels under unprecedented climate conditions. Also, we could only robustly establish the climate-wildfire relationship when evaluated at aggregated spatial and temporal scales; predicting wildfire ignitions and growth at local scales remains very challenging. In the future, combining statistical models that can leverage the observational constraints with process-based climate-vegetation-fire models could likely generate a useful framework for understanding climate impacts on wildfire pollution. Another critical uncertainty is the health effects of smoke $PM_{2.5}$ exposure. Quantifying health impacts of smoke $PM_{2.5}$ at both low and high concentrations in the context of the unique chemical composition of smoke $PM_{2.5}$ and fire influence on human behaviors remains an important area of future research. Furthermore, our estimated health cost is likely only a subset of the overall health burden due to possible morbidity effects of smoke, or health costs from other wildfire-driven pollutants.

Our projections of smoke $PM_{2.5}$ and mortality effects can support climate science, health, and policy research to better understand drivers and consequences of smoke $PM_{2.5}$ under climate change, and help inform policy priorities to address their negative impacts. Our estimates suggest that health costs due to climate-induced smoke $PM_{2.5}$ could be among the most damaging consequences of climate change in the US. Based on our results, designing and implementing policies to reduce wildfire smoke and protect vulnerable communities has the potential to deliver substantial health benefits now and in the coming decades.

Acknowledgments

We thank members of Stanford ECHOLab and Center on Food Security and the Environment, and seminar participants at Brookhaven National Lab for helpful comments. MQ acknowledges the support from the planetary health fellowship at Stanford's Center for Innovation in Global Health. MLC was supported by an Environmental Fellowship at the Harvard University Center for the Environment. Some of the computing for this project was performed on the Stanford Sherlock cluster, and we would like to thank Stanford University and the Stanford Research Computing Center for providing computational resources and support that contributed to these research results. NCEP North American Regional Reanalysis (NARR) data is provided by the NOAA PSL, Boulder, Colorado, USA, from their website at https://psl.noaa.gov.

Author contributions

MQ and MB designed the study. MQ led the smoke projection modeling with inputs from all authors. MQ, JL, RJ led the statistical and machine learning modeling of fire emissions. MQ, SHN, CFG, MLC led the health impacts analysis. MQ and MB led the writing of the manuscript with inputs from all authors. All authors contributed to interpretation of results and reviewed the manuscripts.

Competing interests

The authors declare no competing interests.

Data and materials availability

Data and code to replicate all results in the main text and supplementary materials will be made available at a public repository, except for county-level mortality data for low-population counties, which are not publicly available and were obtained through application to the National Center for Health Statistics.

References

1. V. Iglesias, J. K. Balch, W. R. Travis, US fires became larger, more frequent, and more widespread in the 2000s. *Science advances* **8**, eabc0020 (2022).

2. J. T. Abatzoglou, A. P. Williams, Impact of anthropogenic climate change on wildfire across western US forests. *Proceedings of the National Academy of Sciences* **113**, 11770–11775 (2016).

3. Y. Zhuang, R. Fu, B. D. Santer, R. E. Dickinson, A. Hall, Quantifying contributions of natural variability and anthropogenic forcings on increased fire weather risk over the western United States. *Proceedings of the National Academy of Sciences* **118**, e2111875118 (2021).

4. M. W. Jones *et al.*, Global and regional trends and drivers of fire under climate change. *Reviews of Geophysics* **60**, e2020RG000726 (2022).

5. V. M. Donovan, R. Crandall, J. Fill, C. L. Wonkka, Increasing large wildfire in the eastern United States. *Geophysical Research Letters* **50**, e2023GL107051 (2023).

6. C. D. McClure, D. A. Jaffe, US particulate matter air quality improves except in wildfire-prone areas. *Proceedings of the National Academy of Sciences* **115**, 7901–7906 (2018).

7. K. O'Dell, B. Ford, E. V. Fischer, J. R. Pierce, Contribution of wildland-fire smoke to US PM2. 5 and its influence on recent trends. *Environmental science & technology* **53**, 1797–1804 (2019).

8. M. L. Childs *et al.*, Daily Local-Level Estimates of Ambient Wildfire Smoke PM2. 5 for the Contiguous US. *Environmental Science & Technology* **56**, 13607–13621 (2022).

9. D. Zhang *et al.*, Wildland Fires Worsened Population Exposure to PM2. 5 Pollution in the Contiguous United States. *Environmental Science & Technology* **57**, 19990–19998 (2023).

10. C. E. Reid *et al.*, Critical review of health impacts of wildfire smoke exposure. *Environmental health perspectives* **124**, 1334–1343 (2016).

11. G. Chen *et al.*, Mortality risk attributable to wildfire-related PM2· 5 pollution: a global time series study in 749 locations. *The Lancet Planetary Health* **5**, e579–e587 (2021).

12. C. F. Gould *et al.*, Health effects of wildfire smoke exposure. *Annual Review of Medicine* **75** (2023).

13. S. Heft-Neal *et al.*, Emergency department visits respond nonlinearly to wildfire smoke. *Proceedings of the National Academy of Sciences* **120**, e2302409120 (2023).

14. Y. Li *et al.*, Dominance of wildfires impact on air quality exceedances during the 2020 record-breaking wildfire season in the United States. *Geophysical Research Letters* **48**, e2021GL094908 (2021).

15. M. Burke *et al.*, The changing risk and burden of wildfire in the United States. *Proceedings of the National Academy of Sciences* **118**, e2011048118 (2021).

16. M. Burke *et al.*, The contribution of wildfire to PM2. 5 trends in the USA. *Nature* **622**, 761–766 (2023).

17. N. S. Diffenbaugh, A. G. Konings, C. B. Field, Atmospheric variability contributes to increasing wildfire weather but not as much as global warming. *Proceedings of the National Academy of Sciences* **118**, e2117876118 (2021).

18. A. L. Westerling, Increasing western US forest wildfire activity: sensitivity to changes in the timing of spring. *Philosophical Transactions of the Royal Society B: Biological Sciences* **371**, 20150178 (2016).

19. Z. A. Holden *et al.*, Decreasing fire season precipitation increased recent western US forest wildfire activity. *Proceedings of the National Academy of Sciences* **115**, E8349–E8357 (2018).

20. V. C. Radeloff *et al.*, Rapid growth of the US wildland-urban interface raises wildfire risk. *Proceedings of the National Academy of Sciences* **115**, 3314–3319 (2018).

21. T. M. Ellis, D. M. Bowman, P. Jain, M. D. Flannigan, G. J. Williamson, Global increase in wildfire risk due to climate-driven declines in fuel moisture. *Global change biology* **28**, 1544–1559 (2022).

22. J. K. Balch *et al.*, Warming weakens the night-time barrier to global fire. *Nature* **602**, 442–448 (2022).

23. P. T. Brown *et al.*, Climate warming increases extreme daily wildfire growth risk in California. *Nature* **621**, 760–766 (2023).

24. T. D. Hessilt *et al.*, Future increases in lightning ignition efficiency and wildfire occurrence expected from drier fuels in boreal forest ecosystems of western North America. *Environmental Research Letters* **17**, 054008 (2022).

25. A. A. Gutierrez *et al.*, Wildfire response to changing daily temperature extremes in California's Sierra Nevada. *Science advances* **7**, eabe6417 (2021).

26. J. T. Abatzoglou *et al.*, Projected increases in western US forest fire despite growing fuel constraints. *Communications Earth & Environment* **2**, 227 (2021).

27. S. S.-C. Wang, L. R. Leung, Y. Qian, Projection of future fire emissions over the contiguous US using explainable artificial intelligence and CMIP6 models. *Journal of Geophysical Research: Atmospheres* **128**, e2023JD039154 (2023).

28. Y. Lam, J. Fu, S Wu, L. Mickley, Impacts of future climate change and effects of biogenic emissions on surface ozone and particulate matter concentrations in the United States. *Atmospheric Chemistry and Physics* **11**, 4789–4806 (2011).

29. X. Yue, L. J. Mickley, J. A. Logan, J. O. Kaplan, Ensemble projections of wildfire activity and carbonaceous aerosol concentrations over the western United States in the mid-21st century. *Atmospheric Environment* **77**, 767–780 (2013).

30. Y. Li, L. J. Mickley, P. Liu, J. O. Kaplan, Trends and spatial shifts in lightning fires and smoke concentrations in response to 21st century climate over the national forests and parks of the western United States. *Atmospheric Chemistry and Physics* **20**, 8827–8838 (2020).

31. C. Sarangi *et al.*, Projected increases in wildfires may challenge regulatory curtailment of PM 2.5 over the eastern US by 2050. *Atmospheric Chemistry and Physics Discussions*, 1–30 (2022).

32. J. C. Liu *et al.*, Particulate air pollution from wildfires in the Western US under climate change. *Climatic change* **138**, 655–666 (2016).

33. J. C. Liu *et al.*, Future respiratory hospital admissions from wildfire smoke under climate change in the Western US. *Environmental Research Letters* **11**, 124018 (2016).

34. B. Ford *et al.*, Future fire impacts on smoke concentrations, visibility, and health in the contiguous United States. *GeoHealth* **2**, 229–247 (2018).

35. J. E. Neumann *et al.*, Estimating PM2. 5-related premature mortality and morbidity associated with future wildfire emissions in the western US. *Environmental Research Letters* **16**, 035019 (2021).

36. J. D. Stowell *et al.*, Asthma exacerbation due to climate change-induced wildfire smoke in the Western US. *Environmental Research Letters* **17**, 014023 (2021).

37. E. Grant, J. D. Runkle, Long-term health effects of wildfire exposure: a scoping review. *The Journal of Climate Change and Health* **6**, 100110 (2022).

38. S. S.-C. Wang, Y. Qian, L. R. Leung, Y. Zhang, Interpreting machine learning prediction of fire emissions and comparison with FireMIP process-based models. *Atmospheric Chemistry and Physics* **22**, 3445–3468 (2022).

39. X. Pan *et al.*, Six global biomass burning emission datasets: intercomparison and application in one global aerosol model. *Atmospheric Chemistry and Physics* **20**, 969–994 (2020).

40. T. S. Carter *et al.*, How emissions uncertainty influences the distribution and radiative impacts of smoke from fires in North America. *Atmospheric Chemistry and Physics* **20**, 2073–2097 (2020).

41. X. Ye *et al.*, Evaluation and intercomparison of wildfire smoke forecasts from multiple modeling systems for the 2019 Williams Flats fire. *Atmospheric Chemistry and Physics* **21**, 14427–14469 (2021).

42. X. Huang *et al.*, Smoke-weather interaction affects extreme wildfires in diverse coastal regions. *Science* **379**, 457–461 (2023).

43. Y. Xie, M. Lin, L. W. Horowitz, Summer PM2. 5 pollution extremes caused by wildfires over the western United States during 2017–2018. *Geophysical Research Letters* **47**, e2020GL089429 (2020).

44. R. B. Rice *et al.*, Wildfires Increase Concentrations of Hazardous Air Pollutants in Downwind Communities. *Environmental Science & Technology* **57**, 21235–21248 (2023).

45. Y. Xie *et al.*, Tripling of western US particulate pollution from wildfires in a warming climate. *Proceedings of the National Academy of Sciences* **119**, e2111372119 (2022).

46. S. Hsiang *et al.*, Estimating economic damage from climate change in the United States. *Science* **356**, 1362–1369 (2017).

47. K. Rennert *et al.*, Comprehensive evidence implies a higher social cost of CO2. *Nature* **610**, 687–692 (2022).

48. U.S. Environmental Protection Agency, *Report on the social cost of greenhouse gases: Estimates incorporating recent scientific advances*, 2022.

49. G. R. Van Der Werf *et al.*, Global fire emissions estimates during 1997–2016. *Earth System Science Data* **9**, 697–720 (2017).

50. K. Chen, Y. Ma, M. L. Bell, W. Yang, Canadian wildfire smoke and asthma syndrome emergency department visits in New York City. *JAMA* **330**, 1385–1387 (2023).

51. Y. Ma *et al.*, Wildfire smoke PM2. 5 and mortality in the contiguous United States. *medRxiv* (2023).

52. T. Carleton *et al.*, Valuing the global mortality consequences of climate change accounting for adaptation costs and benefits. *The Quarterly Journal of Economics* **137**, 2037–2105 (2022).

53. U.S. Environmental Protection Agency, *Technical Documentation on the Framework for Evaluating Damages and Impacts (FrEDI)*, 2021.

54. J. A. Kupfer, A. J. Terando, P. Gao, C. Teske, J. K. Hiers, Climate change projected to reduce prescribed burning opportunities in the south-eastern United States. *International Journal of Wildland Fire* **29**, 764–778 (2020).

55. M. Grillakis *et al.*, Climate drivers of global wildfire burned area. *Environmental Research Letters* **17**, 045021 (2022).

56. K. Rao *et al.*, Dry live fuels increase the likelihood of lightning-caused fires. *Geophysical Research Letters* **50**, e2022GL100975 (2023).

57. K. O'Dell *et al.*, Estimated mortality and morbidity attributable to smoke plumes in the United States: not just a western US problem. *GeoHealth* **5**, e2021GH000457 (2021).

58. B. Shrestha, J. A. Brotzge, J. Wang, Observations and Impacts of Long-Range Transported Wildfire Smoke on Air Quality Across New York State During July 2021. *Geophysical Research Letters* **49**, e2022GL100216 (2022).

59. A. Van Donkelaar *et al.*, Monthly global estimates of fine particulate matter and their uncertainty. *Environmental Science & Technology* **55**, 15287–15300 (2021).

60. J. Chen *et al.*, Long-Term Exposure to Low-Level PM 2.5 and Mortality: Investigation of Heterogeneity by Harmonizing Analyses in Large Cohort Studies in Canada, United States, and Europe. *Environmental Health Perspectives* **131**, 127003 (2023).

61. C. A. Pope III, N. Coleman, Z. A. Pond, R. T. Burnett, Fine particulate air pollution and human mortality: 25+ years of cohort studies. *Environmental research* **183**, 108924 (2020).

62. A. Gasparrini *et al.*, Projections of temperature-related excess mortality under climate change scenarios. *The Lancet Planetary Health* **1**, e360–e367 (2017).

63. U.S. Environmental Protection Agency, *Regulatory Impact Analysis for the Clean Power Plan Final Rule*, 2015.

64. M. M. Kelp *et al.*, Prescribed burns as a tool to mitigate future wildfire smoke exposure: Lessons for states and rural environmental justice communities. *Earth's Future* **11**, e2022EF003468 (2023).

65. X. Wu, E. Sverdrup, M. D. Mastrandrea, M. W. Wara, S. Wager, Low-intensity fires mitigate the risk of high-intensity wildfires in California's forests. *Science advances* **9**, eadi4123 (2023).

66. C. L. Schollaert *et al.*, Quantifying the smoke-related public health trade-offs of forest management. *Nature Sustainability*, 1–10 (2023).

67. M. Burke *et al.*, Exposures and behavioural responses to wildfire smoke. *Nature human behaviour* **6**, 1351–1361 (2022).

68. B. Krebs, M. Neidell, Wildfires exacerbate inequalities in indoor pollution exposure. *Environmental Research Letters* (2024).

69. N. W. May, C. Dixon, D. A. Jaffe, *et al.*, Impact of wildfire smoke events on indoor air quality and evaluation of a low-cost filtration method. *Aerosol and Air Quality Research* **21**, 210046 (2021).

70. J. A. Casey *et al.*, Measuring long-term exposure to wildfire PM2. 5 in California: Time-varying inequities in environmental burden. *Proceedings of the National Academy of Sciences* **121**, e2306729121 (2024).

71. K. Rao, A. P. Williams, N. S. Diffenbaugh, M. Yebra, A. G. Konings, Plant-water sensitivity regulates wildfire vulnerability. *Nature ecology & evolution* **6**, 332–339 (2022).

Materials and Methods

Wildfire and smoke $PM_{2.5}$ datasets

We use annual fire emissions from the fourth version of the Global Fire Emissions Database with small fires (GFED4s) from 2001-2021 (*1*). The native spatial resolution of GFED4s is 0.25×0.25 degrees. We use the estimated dry matter (DM) emissions as our primary variable for the emissions. DM emissions capture the amount of biomass being consumed in the burning process. We choose DM emissions as the proxy for overall fire emissions (rather than individual emissions species such as black carbon or NO_x) due to uncertainty in the emission factors used in GFED4s. GFED4s include fire emissions from agriculture fires and land-use change as well. However, as wildland fire emissions dominate in most study regions (especially in western US and Canada where we see the largest effects), we refer to our estimates as "wildfire emissions" and "wildfire smoke" for simplicity and consistency (Table S1).

For smoke $PM_{2.5}$, we use gridded daily wildfire smoke $PM_{2.5}$ predictions for the contiguous US at 10 km resolution from January 1, 2006 to December 31, 2020 derived from (*2*). This dataset specifically estimates the ambient $PM_{2.5}$ concentration due to wildfire smoke influence by constructing a machine learning model that uses smoke plume data, remotely-sensed variables, and meteorological variables to predict the anomalous increases in surface $PM_{2.5}$ measured by surface air quality monitors during wildfire. To estimate contributions of smoke $PM_{2.5}$ to total $PM_{2.5}$, we use the total $PM_{2.5}$ estimates from (*3*), which combines satellite retrievals of aerosol optical depth, chemical transport modeling, and ground-based measurements to estimate monthly total ambient $PM_{2.5}$ concentrations.

Climate and meteorological datasets

We use climate and land use variables to predict wildfire DM emissions. The climate variables include 2m air temperature, precipitation, relative humidity, soil moisture (of the top soil layer), vapor pressure deficit (VPD), wind speed (at 10m level), and runoff (sum of surface and subsurface). We include these climate variables because they are available in both the historical data and the climate projections from CMIP6 climate model ensembles. Our models do not include other potentially important variables such as fire weather index and fuel moisture (as used in (*4*)) because they are unavailable in future projections. These climate variables are derived from the North American Regional Reanalysis (NARR) (*5*), with the exception of soil moisture. Soil moisture is derived from the VIC land-surface model of phase 2 of the North American Land Data Assimilation System (NLDAS-2) (*6*) and only available in the contiguous US. The native spatial resolution is 32 km for NARR variables and 0.125 degree for NLDAS-2 variables. Land use variables are derived from the North American Land Change Monitoring System (NALCMS) for the year 2015 (*7*). More specifically, we use three land use variables which each represents the percentage of area in three categories: cropland, forest, and grassland. The native resolution of land use variables is 30m. Because high-resolution projections of future land use change are not available, the land use variables are held constant across time in both the historical and future periods.

For future climate change scenarios, we use the projected climate variables from the Coupled Model Intercomparison Project Phase 6 (CMIP6). We examine three primary climate-forcing scenarios featured by the IPCC, which are constructed as pairs between the Shared Socio-economic Pathways (SSPs) and the Representative Concentration Pathways (RCPs) (*8*). We use SSP1-2.6 (which the IPCC refers to as the "Low" scenario), SSP2-4.5 (which the IPCC refers to as the "Intermediate" scenario), and SSP3-7.0 (which the IPCC refers to as the "High" scenario). We use projections from 28 global climate models that include the selected variables that cover the study region (Table S6). Following practice of IPCC, we select only one ensemble realization for each model – we use the first ensemble variant of each model ("r1i1p1f1") when possible.

When modeling the relationship between wildfire emissions and smoke $PM_{2.5}$, we also include meteorological variables in the regression model. The daily gridded meteorological variables are derived from gridMET (*9*). In our main specification, we aggregate the meteorological variable to the monthly and smoke grid cell level. We include the splines of daily surface temperature, precipitation, dewpoint temperature, boundary layer height, air pressure, 10m wind direction (U and V components) and wind speed.

Predicting wildfire emissions

We construct an ensemble of statistical and machine learning models to predict wildfire emissions using climate and land use variables. Our models predict the annual dry matter (DM) emissions derived from GFED4s emission inventory using climate and land-use variables from 2001 to 2021. We build separate models for each of the five regions (western US, southeastern US, northeastern US, Canada-Alaska, and Mexico) to capture the regionally heterogeneous relationships between climate, land type and wildfire emissions. For each region, we construct six different models as potential model candidates: linear regression model, linear regression model with log outcomes, Least Absolute Shrinkage and Selection Operator (LASSO) models, LASSO models with log outcomes, 2-layer Neural Network (NN) model, and NN models with log outcomes. These six algorithms are selected to cover a possible range of model candidates with varying desired characteristics – including simple models that are commonly used in prior studies (e.g., the linear and log-linear regression models), models that are easy to interpret (e.g., the linear regression and LASSO models), and more flexible machine learning models that are used in prior studies (e.g., the NN model).

One key challenge for this prediction problem is that the fire occurrence, spread, and resulting emissions at local scales are often fairly stochastic due to varying and hard-to-predict non-climate factors, including where and when human and natural ignitions occur and how much suppression effort is applied. Therefore, to better capture the predictable components of the climate-wildfire relationship, we create models to predict annual emissions aggregated at different spatial scales for each of the six model types mentioned above. We aggregate the outcome variables and model features at four spatial scales: the grid scale (0.25 deg, 26956 cells in total), the North America Level-3 Ecoregion scale (177 regions in total), the North America Level-2 Ecoregion scale (51 regions in total), and the regional scale (5 regions in total). We then select the spatial resolution that optimizes model performance for each model type (as described below), allowing the optimal spatial resolution to differ across different model types and regions (see Figure S3 for model performances across spatial scales).

To evaluate the model performance, we use nested leave-one-out cross-validations (LOOCV) at the temporal scale. We divide our data into 21 temporal folds, each including one year of data. For each holdout fold, we train the model using the remaining 20 folds of data with hyper-parameters selected using an inner-loop 5-fold CV within the training data. We then obtain out-of-sample predictions for the holdout fold and repeat this process to obtain out-of-sample predictions for the entire time period. As we focus on projecting the future wildfire emissions over a 10-year period (i.e. decadal averages) under future climate scenarios, we thus evaluate the performance of our models on similar 10-year intervals. We compute the moving averages of predicted and observed emissions over 10-year moving windows. We compute two metrics and use them as the basis for evaluating the performance of each model: 1) the root mean square error between predictions and observations, and 2) the prediction biases of the highest-emitting 10-year period. The first metric allows us to assess the model performance across years with different climate conditions to detect differences between current and future climate for different climate scenarios. The second metric allows us to assess the model performance under the extreme smoke conditions which are more likely to occur under future climate. To obtain the final model that can be used for future projections, we create an "ensemble model" which combines the predictions from the selected base models with the corresponding optimal spatial resolution. The selected models and their performances can be found in Table S2.

Quantifying fire impacts on smoke $PM_{2.5}$

To estimate smoke $PM_{2.5}$ concentrations associated with future wildfire emissions, we design a statistical approach to establish an empirical relationship between ambient smoke $PM_{2.5}$ from (*2*) and wildfire emissions derived from GFED4s. We estimate the relationship between wildfire emissions and smoke $PM_{2.5}$ concentration across the contiguous US (48 states and the District of Columbia) at 10 km resolution, accounting for variation in wind directions and atmospheric transport. This approach allows us to efficiently predict smoke concentration in one location from changes in wildfire emissions in another. Despite using estimated DM emissions from GFED4s as an input, our estimates of smoke $PM_{2.5}$ concentrations strongly predict the variations in the empirical estimates of surface smoke $PM_{2.5}$ concentrations, and are thus directly constrained by surface $PM_{2.5}$ measurement during wildfire episodes.

Specifically, we use the following regression equation to empirically quantify the impacts of the wildfire DM emissions on smoke $PM_{2.5}$ in the US in our historical data:

$$Smoke_{iym} = \sum_{d,w} \beta_{dw} \Delta Emis_{dw,iym} + \gamma \boldsymbol{W_{iym}} + \eta y + \psi_m + \theta_i + \epsilon_{iym} \tag{1}$$

where $Smoke_{iym}$ denotes the smoke $PM_{2.5}$ at grid cell i (resolution: 10 km), year y and month-of-year m. $Emis_{dw,iym}$ denotes the wildfire DM emissions that in the distance bin d and wind direction w ($w \in \{upwind, other, downwind\}$) of the smoke location i on month-of-year m and year y. In our main specification, we estimate the impacts of wildfire DM emissions at different distances from the smoke location: *<50 km, 50-100 km, 100-200 km, 200-350 km, 350-500 km, 500-750 km, 750-1000 km, 1000-1500 km, 1500-2000 km, >2000 km*. $\boldsymbol{W_{iym}}$ are the meteorological variables at the grid cell i (as described in the dataset section). We include these meteorological variables to capture potential meteorological variability that could influence ambient $PM_{2.5}$ concentrations. Our main specification includes linear year trend (ηy) and month-of-year fixed effects (ψ_m) to capture the long-term trend and seasonality of smoke $PM_{2.5}$ concentration, and grid cell-level fixed effects (θ_i) to control for the time-invariant unobserved factors at the grid cell location. ϵ_{iym} represents the error term.

To better capture the atmospheric transport of smoke $PM_{2.5}$, we divide the wildfire emissions (from a given distance bin) into three categories depending on wind direction and the location of fire. Following methods in (*10*), wildfire emissions are classified into "upwind" or "downwind", depending on whether the wildfire location is at the upwind or downwind direction of the smoke grid cell. We combine daily emissions with daily wind direction (10m wind) to calculate the daily emission from each wind direction and further aggregate to the monthly level.

Many previous studies have demonstrated that wildfire emission factors (e.g., mass of organic carbon particles emitted from burning one kg fuel) strongly depend on the combustion conditions (e.g., the combustion completeness) and the underlying fuel type among many other factors (*11–14*). As many of these characteristics (e.g., the combustion efficiency of different fires) are not available at the national scale, we use a data-driven approach and estimate different models/equations for the nine US climate regions determined by National Centers for Environmental Information (see Figure 2 for region definitions), which allows the relationship between emissions and surface smoke $PM_{2.5}$ to differ by region. The resulting regional estimates therefore implicitly account for some heterogeneity in the vegetation fuel types, fire intensities (as characterized in historical fires), and topographies for different locations. For example, prior studies have shown that smoldering fires often have higher $PM_{2.5}$ emission factors compared to flaming fires due to incomplete combustion (*13*), which might partly explain the relatively high emissions factors in the Southeast as smoldering fires are more common there due to high humidity (*15*).

Projecting wildfire emissions and smoke $PM_{2.5}$ under future climate

We combine our ensemble of statistical and machine learning models with climate projections from ensembles of global climate models to project the wildfire emissions and smoke $PM_{2.5}$ under future climate scenarios. Consistent with the optimal spatial resolutions selected for each region, we predict the annual wildfire DM emissions at different spatial resolutions, from 2001-2055. We then statistically downscale the predicted regional emissions to the native grid cell level (0.25 degree) by distributing predicted DM emissions using average historical spatial distribution of emissions at the grid cell level (2001-2021).

We combine the downscaled predicted DM emissions at GFED4s grid cell level (0.25 degree) with the empirical relationship we established between smoke $PM_{2.5}$ and GFED4s DM emissions to calculate predicted smoke $PM_{2.5}$ in each smoke grid cell (resolution of 10 km). When calculating the smoke $PM_{2.5}$ in future scenarios, the wind direction and meteorological conditions are held constant at the average conditions in the historical period. We further calculate the difference between the estimated smoke in any future year and the average *estimated* smoke between 2011-2020. The delta difference is then added to the average *observed* smoke $PM_{2.5}$ concentration between 2011-2020 to obtain the final smoke predictions for each grid cell in the future years.

Impacts of smoke $PM_{2.5}$ on mortality

We calculate all-cause mortality associated with wildfire smoke exposure historically and under future climate scenarios using a dose-response function empirically derived from 2006-2019 county-level data. We combine county-level population-weighted annual smoke $PM_{2.5}$, derived from (*2*), with county-level all-cause mortality rates by different age groups. We obtain individual-level multiple cause of death mortality data from the National Center for Health Statistics to calculate age-standardized mortality rates for all ages, those under 65 years of age, and those 65 years and older (*16*). County-level mortality rates were age-standardized using the direct method and 5-year bins (0-4, 5-9, ..., 85 and over) based on the 2000 US Census Standard Population. Monthly mortality rates were standardized per 100,000 population. To fully capture damages from ambient wildfire smoke concentrations, our preferred outcome is age-standardized, all-cause, all-age mortality rates at the county-year level. We also separately estimate impacts among those 65 years and older and those under 65 years of age (Figure S6).

In our main analysis, we estimate a Poisson model in which we allow non-linear impacts of annual smoke $PM_{2.5}$ on mortality rates at the county-year level:

$$D_{csy} = \exp\,(\sum_i \beta_i smokeBIN^i_{csy} + \gamma W_{csy} + \eta_{sy} + \theta_c + \varepsilon_{csy}) \tag{2}$$

where D_{csy} denotes the age-adjusted all-cause mortality rates in county c, state s, and year y. $smokeBIN^i_{csy}$ is a dummy variable for whether annual population-weighted smoke $PM_{2.5}$ in county c, state s, and year y falls into the range of bin i (0-0.1, 0.1-0.25, 0.25-0.5, 0.5-0.75, 0.75-1, 1-2, 2-3, 3-4, 4-5, 5-6, >6 μg/m^3; 0-0.1 is the reference category). The main coefficients of interest are the β_i's, which estimate the effects of a year with annual smoke concentration of bin i on mortality rates, relative to a year with annual mean smoke $PM_{2.5}$ concentration below 0.1 μg/m^3. The reference category included <0.1 because only 4 county-year observations had exactly zero ambient wildfire smoke. W_{csy} denotes a flexible control of temperature (the number of days that fall in different temperature bins) and linear and quadratic terms of annual population-weighted precipitation. η_{sy} denotes a vector of state-year fixed effects (i.e. separate intercepts for each year in each state) that accounts for all factors that differ across states in a given year (e.g. California 2018 versus Oregon 2018) as well as all factors that differ within states across years (e.g. California 2017 versus California 2018). θ_c denotes a set of county-level fixed effects that accounts for any county-specific time-invariant factors that could be correlated with both smoke exposure and mortality (e.g., high income communities in the mountainous areas on the west coast could have higher smoke exposure but lower mortality rates due to non-smoke reasons). In essence, we identify the effect of wildfire smoke on mortality using within-county variation over time, after accounting for any factors that trend over time within that county's state, and for any correlation between smoke variation and variation in temperature and precipitation. Because temporal variation in wildfire smoke exposure is largely a function of idiosyncratic factors such as where a given fire starts and which way the wind blows, our estimates have a plausibly causal interpretation. The coefficients are estimated using weighted Poisson regression models, with function "fepois" from R package "fixest". The estimations are weighted by county-level population counts to enable estimates of population-averaged effects, as well as to reduce statistical uncertainty. The uncertainty of the coefficients are estimated using bootstrap of 500 runs. ϵ_{csy} represents the error terms.

While we observe historical data on daily smoke $PM_{2.5}$ concentrations and monthly cause-specific mortality rates, we estimate the dose-response functions at the annual level to be consistent with our smoke concentration projections, which are only feasible at the annual level. This approach deviates from previous studies estimating health impacts from wildfire smoke which focus primarily on sub-annual exposures, but it allows for a direct application of the estimated response functions to annual smoke projections. It also has the advantage of allowing us to capture the net effect of either behavioral dynamics in response to short-term variation, as has been observed in related settings (*17*), or "displacement" of mortality that would of otherwise occurred but was hastened as a result of short-term exposure – a common concern in climate impact studies (*18*).

To evaluate the influence of functional forms of the dose-response function, we estimate alternative response functions using a Poisson model, a least-squares linear regression, and a quadratic model where wildfire smoke concentrations were treated as a continuous exposure, and calculate how different functional forms influence the estimates of projected annual excess deaths (Figure S9). We find that non-binned models generally fail to capture meaningful impacts of both low-level and high-level smoke exposure (Figure S12).

Further, to assess the sensitivity of our results to multiple assumptions, we estimate several alternative specifications of the Poisson model. Specifically, we estimate a model which uses alternative bin definitions, a model which includes year 2020, a model which calculates the number of months or the number of days in a year that fall in different smoke bins to represent different temporal aggregations, and a model which is estimated at county-month level. While we cannot calculate the impact on projected mortality under scenarios using these sub-annual measures of wildfire smoke $PM_{2.5}$ given the resolution of the wildfire smoke projections, we instead compare between estimated historical excess deaths during 2011-2020, calculated as the difference between predicted deaths at observed smoke levels relative to what would have occurred absent any smoke. We find that the largest differences occur when using monthly bins, likely due to the lagged effects of smoke on mortality at the monthly level (Figure S10).

To calculate smoke attributable deaths in the historical scenario, we use the county-level population data for the year 2019. We use the county-level average death rate between 2006 to 2019 as the baseline mortality rate for calculations with the Poisson model. For projections of future mortality burden, we scale the population according to the future population projections from the US Census (*19*).

Monetizing health impacts

The mortality impacts are monetized using a value of statistical life (VSL) of $10.95 million (year 2019 dollars), as recommended by the US EPA (*20*) and used in previous studies (*21*). For future scenarios, we adjust VSL values using the projected economic growth of 2% and income elasticity of one, following a similar method from Carleton et al. (*21*). We compare the monetized health impacts from climate-induced smoke with two prior estimates of aggregate monetized/economic damage due to climate change. Hsiang et al. estimated an annual damage of 0.4%-0.8% of US GDP or $166-332 billion (in year 2019 dollars, using annual projected GDP of $38.5 trillion from (*22*)). Their approach empirically calculated the effects of climate change on a variety of economic damages from temperature-related mortality, agriculture, crime, coastal storms, energy, and labor channels (*23*). The Framework for Evaluating Damages and Impacts (FrEDI), developed by US EPA (*22*), estimated an annual damage of $292 billion in the 2050s. FrEDI considered 21 sectors (including estimated wildfire damages from western US (*24*)). The wildfire health damages considered in FrEDI only accounted for effects of wildfire in the western US and used an empirical climate-fire relationship derived from historical data before 2013 which did not include recent extreme wildfire years (*24*). We use the default parameters and results from FrEDI in the year of 2050.

References for Methods

1. G. R. Van Der Werf *et al.*, Global fire emissions estimates during 1997–2016. *Earth System Science Data* **9**, 697–720 (2017).

2. M. L. Childs *et al.*, Daily Local-Level Estimates of Ambient Wildfire Smoke PM2. 5 for the Contiguous US. *Environmental Science & Technology* **56**, 13607–13621 (2022).

3. A. Van Donkelaar *et al.*, Monthly global estimates of fine particulate matter and their uncertainty. *Environmental Science & Technology* **55**, 15287–15300 (2021).

4. J. Buch, A. P. Williams, C. S. Juang, W. D. Hansen, P. Gentine, SMLFire1. 0: a stochastic machine learning (SML) model for wildfire activity in the western United States. *Geoscientific Model Development* **16**, 3407–3433 (2023).

5. F. Mesinger *et al.*, North American regional reanalysis. *Bulletin of the American Meteorological Society* **87**, 343–360 (2006).

6. Y. Xia *et al.*, Continental-scale water and energy flux analysis and validation for the North American Land Data Assimilation System project phase 2 (NLDAS-2): 1. Intercomparison and application of model products. *Journal of Geophysical Research: Atmospheres* **117** (2012).

7. Produced by Natural Resources Canada/ The Canada Centre for Mapping and Earth Observation (NRCan/CCMEO), United States Geological Survey (USGS); Instituto Nacional de Estadística y Geografía (INEGI), Comisión Nacional para el Conocimiento y Uso de la Biodiversidad (CONABIO) and Comisión Nacional Forestal (CONAFOR), *2015 North American Land Cover at 30 m spatial resolution.*

8. IPCC, in *Climate Change 2021: The Physical Science Basis. Contribution of Working Group I to the Sixth Assessment Report of the Intergovernmental Panel on Climate Change*, ed. by V. Masson-Delmotte *et al.* (Cambridge University Press, Cambridge, United Kingdom and New York, NY, USA, 2021), 3−32.

9. J. T. Abatzoglou, Development of gridded surface meteorological data for ecological applications and modelling. *International Journal of Climatology* **33**, 121–131 (2013).

10. M. Qiu, N. Ratledge, I. M. Azevedo, N. S. Diffenbaugh, M. Burke, Drought impacts on the electricity system, emissions, and air quality in the western United States. *Proceedings of the National Academy of Sciences* **120**, e2300395120 (2023).

11. S. Urbanski, Wildland fire emissions, carbon, and climate: Emission factors. *Forest Ecology and Management* **317**, 51–60 (2014).

12. C. N. Jen *et al.*, Speciated and total emission factors of particulate organics from burning western US wildland fuels and their dependence on combustion efficiency. *Atmospheric Chemistry and Physics* **19**, 1013–1026 (2019).

13. Y. Liang *et al.*, Emissions of Organic Compounds from Western US Wildfires and Their Near Fire Transformations. *Atmospheric Chemistry and Physics Discussions*, 1–32 (2022).

14. D. A. Jaffe *et al.*, Wildfire and prescribed burning impacts on air quality in the United States. *Journal of the Air & Waste Management Association* **70**, 583–615 (2020).

15. G. L. Achtemeier, Measurements of moisture in smoldering smoke and implications for fog. *International Journal of Wildland Fire* **15**, 517–525 (2006).

16. National Center for Health Statistics Division of Vital Statistics, *NVSS Restricted-use Mortality Files, 1999-2021. Hyattsville, Maryland.*

17. S. Heft-Neal *et al.*, Emergency department visits respond nonlinearly to wildfire smoke. *Proceedings of the National Academy of Sciences* **120**, e2302409120 (2023).

18. S. Hsiang, Climate econometrics. *Annual Review of Resource Economics* **8**, 43–75 (2016).

19. U.S. Census Bureau, *2023 National Population Projections Tables: Main Series*, 2023.

20. U.S. Environmental Protection Agency, *Regulatory Impact Analysis for the Clean Power Plan Final Rule*, 2015.

21. T. Carleton *et al.*, Valuing the global mortality consequences of climate change accounting for adaptation costs and benefits. *The Quarterly Journal of Economics* **137**, 2037–2105 (2022).

22. U.S. Environmental Protection Agency, *Technical Documentation on the Framework for Evaluating Damages and Impacts (FrEDI)*, 2021.

23. S. Hsiang *et al.*, Estimating economic damage from climate change in the United States. *Science* **356**, 1362–1369 (2017).

24. J. E. Neumann *et al.*, Estimating PM2. 5-related premature mortality and morbidity associated with future wildfire emissions in the western US. *Environmental Research Letters* **16**, 035019 (2021).

25. J. T. Abatzoglou, A. P. Williams, Impact of anthropogenic climate change on wildfire across western US forests. *Proceedings of the National Academy of Sciences* **113**, 11770–11775 (2016).

26. S. S.-C. Wang, Y. Qian, L. R. Leung, Y. Zhang, Interpreting machine learning prediction of fire emissions and comparison with FireMIP process-based models. *Atmospheric Chemistry and Physics* **22**, 3445–3468 (2022).

Supplementary tables

Table S1: Estimated dry matter (DM) emissions by land-use type in historical period and future scenarios. For the historical period, the table shows the annual mean DM emissions from each land-use type in each region from 2001-2021, directly derived from GFED4s. For the future scenario, the table shows the annual mean DM emissions from each land-use type in each region under SSP3-7.0 from 2046-2055. Landuse types are derived from GFED4s inventory. "Forest" includes emissions from both temperate forests and boreal forests.

Region	Type	2001 - 2021		2050 SSP3-7.0
		emissions (MT)	percent	emissions (MT)
Western US	forest	25.8	68%	184.7
	savanna	10.7	28%	76.5
	agriculture	1.7	4%	12.3
	landuse change	0.0	0%	0.0
	peatland	0.0	0%	0.0
Southeastern US	forest	4.2	28%	4.4
	savanna	5.3	35%	5.8
	agriculture	5.6	37%	5.6
	landuse change	0.0	0%	0.0
	peatland	0.0	0%	0.0
Northeastern US	forest	0.6	29%	0.6
	savanna	0.2	11%	0.2
	agriculture	1.2	60%	1.1
	landuse change	0.0	0%	0.0
	peatland	0.0	0%	0.0
Canada-Alaska	forest	152.6	94%	240.8
	savanna	0.2	0%	0.4
	agriculture	1.7	1%	2.7
	landuse change	0.0	0%	0.0
	peatland	8.2	5%	13.0
Mexico	forest	1.2	3%	1.7
	savanna	19.4	47%	29.0
	agriculture	6.4	16%	9.5
	landuse change	14.1	34%	17.1
	peatland	0.0	0%	0.0

Table S2: Performance of the individual statistical and machine learning models. For each region, we train six algorithms {Linear, LASSO, Neural Net} $\times$ {level, log of the outcome}. The table shows the optimal spatial resolution and three evaluation metrics for each algorithm. The three evaluation metrics are correlation coefficient (R), bias in predicting the highest-emitting 10-year (Bias), and Root Mean Square Error over the mean of the outcome (RMSE/Mean). Bias is calculated as *(Prediction - Observation) / Observation* for the 10-year period with the highest emissions. Models selected in the final model ensembles are bolded and labeled "Y" in the "Selected" column. The selection is based on RMSE + |Bias| to consider both metrics. In our main analysis, for each region, only the algorithms with "RMSE + |Bias|" within 5% of the best algorithm are selected.

Region	Algorithm	Optimal resolution	R	Bias	RMSE/ Mean	RMSE + |Bias|	Diff	Selected
Western US	**Linear, level**	**regional**	**0.98**	**-10%**	**20%**	**29%**	**0%**	**Y**
Western US	Linear, log	eco2	0.91	-16%	22%	37%	8%	N
Western US	LASSO, level	regional	0.99	-14%	28%	43%	13%	N
Western US	**LASSO, log**	**regional**	**0.89**	**-3%**	**31%**	**33%**	**4%**	**Y**
Western US	Neural Net, level	eco2	0.73	0%	90%	91%	61%	N
Western US	Neural Net, log	eco3	0.98	-20%	19%	39%	9%	N
Southeastern US	**Linear, level**	**eco3**	**0.51**	**-1%**	**6%**	**7%**	**0%**	**Y**
Southeastern US	Linear, log	eco2	0.36	-18%	14%	32%	25%	N
Southeastern US	LASSO, level	eco2	0.58	-12%	9%	21%	14%	N
Southeastern US	LASSO, log	eco2	0.02	-16%	14%	30%	23%	N
Southeastern US	Neural Net, level	grid	0.11	5%	11%	16%	9%	N
Southeastern US	Neural Net, log	eco2	0.30	-12%	12%	24%	17%	N
Northeastern US	**Linear, level**	**grid**	**0.05**	**-2%**	**11%**	**13%**	**0%**	**Y**
Northeastern US	Linear, log	regional	0.06	-11%	9%	20%	7%	N
Northeastern US	LASSO, log	eco2	0.19	-26%	19%	45%	32%	N
Northeastern US	**Neural Net, level**	**eco2**	**0.07**	**2%**	**14%**	**15%**	**2%**	**Y**
Northeastern US	Neural Net, log	eco3	0.29	-20%	12%	32%	20%	N
Canada-Alaska	**Linear, level**	**regional**	**0.91**	**4%**	**15%**	**19%**	**0%**	**Y**
Canada-Alaska	Linear, log	eco2	0.70	43%	35%	78%	59%	N
Canada-Alaska	LASSO, level	eco2	0.94	-15%	19%	34%	15%	N
Canada-Alaska	LASSO, log	regional	0.73	-13%	16%	29%	10%	N
Canada-Alaska	Neural Net, level	eco3	0.20	-9%	27%	36%	17%	N
Canada-Alaska	Neural Net, log	regional	0.71	-30%	15%	45%	26%	N
Mexico	**Linear, level**	**eco2**	**0.88**	**0%**	**4%**	**4%**	**0%**	**Y**
Mexico	Linear, log	eco2	0.85	-2%	14%	16%	12%	N
Mexico	**LASSO, level**	**eco3**	**0.86**	**0%**	**5%**	**5%**	**1%**	**Y**
Mexico	LASSO, log	eco2	0.71	-13%	14%	27%	23%	N
Mexico	Neural Net, level	eco2	0.72	0%	10%	10%	6%	N
Mexico	Neural Net, log	regional	0.82	-7%	7%	14%	9%	N

Table S3: Estimated coefficients from the selected linear regression models that use climate features to predict wildfire emissions. The table only shows the coefficients from the final selected models in each region with the corresponding optimal spatial resolution. Statistically significant coefficients ($p < 0.1$) are bolded.

	Western US		Southeastern US		Northeastern US		Canada-Alaska		Mexico	
	coef	p-value	coef	p-value	coef	p-value	coef	p-value	coef	p-value
temperature	2.0E-02	0.25	-9.9E-04	0.15	2.1E-04	0.30	-3.0E-02	0.08	**-1.2E-02**	**0.00**
precipitation	-3.3E-02	0.27	**-4.9E-03**	**0.00**	-2.5E-04	0.63	-3.6E-02	0.43	**8.8E-03**	**0.00**
RH	5.6E-03	0.26	2.4E-04	0.55	-1.2E-04	0.36	2.3E-02	0.23	**4.8E-03**	**0.00**
wind speed	7.3E-02	0.12	**9.6E-03**	**0.00**	**-1.6E-03**	**0.09**	4.6E-02	0.79	-1.1E-03	0.92
VPD	-2.3E-02	0.94	3.3E-03	0.74	-2.5E-03	0.55	**2.4E+00**	**0.02**	**2.6E-01**	**0.00**
runoff	1.2E-02	0.24	5.5E-04	0.83	5.1E-04	0.49	1.2E-01	0.13	-9.1E-03	0.26
soil moisture	**-2.6E-02**	**0.01**	**-3.8E-03**	**0.00**	-2.8E-04	0.51				

Table S4: Estimated coefficients from the selected LASSO models that use climate features to predict wildfire emissions. As LASSO models are only selected in the western US and Mexico, the table shows the coefficients from these two final selected models with the corresponding optimal spatial resolution.

Western US		Mexico	
Selected variables	coef	Selected variables	coef
soil moisture	-1.2E+00	VPD*grass	4.1E-01
temperature	1.1E+00	VPD*precipitation	9.0E-03
VPD*precipitation	-2.8E+00	VPD*RH	1.3E-03
VPD*runoff	2.5E+00		
RH^2	-1.5E-04		
runoff^2	-1.6E-01		
runoff*wind speed	1.3E-02		
temperature^2	4.6E-05		
wind speed^2	4.1E-01		

Table S5: Estimated population-weighted average smoke $PM_{2.5}$, total $PM_{2.5}$, and smoke $PM_{2.5}$ contribution at the state level. Total $PM_{2.5}$ are calculated as the sum of smoke and non-smoke $PM_{2.5}$ concentrations. Non-smoke $PM_{2.5}$ are assumed to be the same as the average non-smoke $PM_{2.5}$ between 2016-2020, calculated as the difference between total $PM_{2.5}$ from (*3*) and smoke $PM_{2.5}$ from (*2*). Only states with >10% smoke contributions under SSP3-7.0 scenario are listed.

State	Smoke $PM_{2.5}$ $\mu g/m^3$	Total $PM_{2.5}$ $\mu g/m^3$	Smoke percent	State	Smoke $PM_{2.5}$ $\mu g/m^3$	Total $PM_{2.5}$ $\mu g/m^3$	Smoke percent	Scenario
Oregon	1.3	6.6	20%	Kansas	0.7	7.3	9%	2011-2020
	5.0	9.7	51%		1.5	7.7	19%	SSP1-2.6
	6.2	11.0	57%		1.7	7.9	21%	SSP2-4.5
	7.5	12.3	61%		1.8	8.1	22%	SSP3-7.0
Montana	1.3	6.4	20%	Nebraska	0.7	7.4	9%	2011-2020
	4.7	9.7	48%		1.2	7.4	16%	SSP1-2.6
	5.7	10.7	53%		1.3	7.5	18%	SSP2-4.5
	6.9	11.9	58%		1.5	7.6	19%	SSP3-7.0
Washington	0.9	6.0	16%	Oklahoma	0.6	7.8	8%	2011-2020
	3.8	8.3	46%		1.2	8.0	15%	SSP1-2.6
	4.6	9.0	51%		1.4	8.2	17%	SSP2-4.5
	5.6	10.0	56%		1.5	8.3	19%	SSP3-7.0
Idaho	1.3	7.1	18%	Minnesota	0.6	6.6	9%	2011-2020
	4.4	10.0	44%		0.9	6.5	14%	SSP1-2.6
	5.4	11.0	49%		1.0	6.7	15%	SSP2-4.5
	6.4	12.0	54%		1.1	6.8	16%	SSP3-7.0
Wyoming	0.7	5.4	13%	Arkansas	0.6	8.2	7%	2011-2020
	2.6	7.1	37%		1.1	8.0	14%	SSP1-2.6
	3.2	7.7	42%		1.2	8.2	15%	SSP2-4.5
	3.9	8.4	47%		1.3	8.2	16%	SSP3-7.0
Nevada	0.5	7.0	7%	Texas	0.5	8.3	6%	2011-2020
	3.1	9.6	32%		1.1	8.5	12%	SSP1-2.6
	3.9	10.4	38%		1.2	8.6	14%	SSP2-4.5
	4.6	11.1	42%		1.3	8.7	15%	SSP3-7.0
North Dakota	0.7	5.3	14%	Arizona	0.2	8.2	2%	2011-2020
	1.7	6.1	28%		0.9	8.7	11%	SSP1-2.6
	2.0	6.3	31%		1.1	8.9	13%	SSP2-4.5
	2.2	6.5	33%		1.3	9.1	14%	SSP3-7.0
California	0.6	10.5	6%	Iowa	0.6	7.8	8%	2011-2020
	2.8	12.2	23%		0.8	7.5	11%	SSP1-2.6
	3.5	12.9	27%		0.9	7.6	12%	SSP2-4.5
	4.1	13.5	30%		1.0	7.7	13%	SSP3-7.0
Colorado	0.5	6.1	9%	Wisconsin	0.5	7.4	7%	2011-2020
	1.7	7.2	24%		0.8	7.1	11%	SSP1-2.6
	2.0	7.5	27%		0.9	7.3	12%	SSP2-4.5
	2.3	7.8	30%		1.0	7.3	13%	SSP3-7.0
Utah	0.5	6.9	7%	Louisiana	0.4	8.5	5%	2011-2020
	1.7	7.7	22%		0.8	8.5	10%	SSP1-2.6
	2.0	8.0	26%		1.0	8.6	11%	SSP2-4.5
	2.4	8.4	29%		1.0	8.6	12%	SSP3-7.0
South Dakota	0.7	6.1	11%	Mississippi	0.4	8.3	5%	2011-2020
	1.4	6.3	22%		0.7	8.0	9%	SSP1-2.6
	1.5	6.5	24%		0.9	8.1	11%	SSP2-4.5
	1.7	6.7	26%		0.9	8.2	11%	SSP3-7.0
New Mexico	0.3	5.4	6%	Michigan	0.4	8.0	5%	2011-2020
	1.2	6.0	20%		0.6	7.6	8%	SSP1-2.6
	1.4	6.2	23%		0.7	7.7	9%	SSP2-4.5
	1.6	6.4	25%		0.8	7.7	10%	SSP3-7.0

Table S6: Climate models used in this study for future projections. We use projections from 28 global climate models with available output under the historical and three climate scenarios from the CMIP6 model ensembles. The spatial resolution of each model is shown in latitude $\times$ longitude (unit: degree). Resolutions are approximated for models with varying latitudes. Data is downloaded in February, 2023.

Model	**Ensemble variant**	**Resolution**
ACCESS-CM2	r1i1p1f1	1.25 x 1.88
ACCESS-ESM1-5	r1i1p1f1	1.25 x 1.88
BCC-CSM2-MR	r1i1p1f1	1.12 x 1.12
CanESM5	r1i1p1f1	2.79 x 2.81
CAS-ESM2-0	r1i1p1f1	1.42 x 1.41
CESM2-WACCM	r1i1p1f1	0.94 x 1.25
CMCC-CM2-SR5	r1i1p1f1	0.94 x 1.25
CMCC-ESM2	r1i1p1f1	0.94 x 1.25
CNRM-CM6-1	r1i1p1f2	1.4 x 1.41
CNRM-CM6-1-HR	r1i1p1f2	0.5 x 0.5
CNRM-ESM2-1	r1i1p1f2	1.4 x 1.41
EC-Earth3	r1i1p1f1	0.7 x 0.7
EC-Earth3-Veg	r1i1p1f1	0.7 x 0.7
EC-Earth3-Veg-LR	r1i1p1f1	1.12 x 1.12
FGOALS-f3-L	r1i1p1f1	0.94 x 1.25
FGOALS-g3	r1i1p1f1	2.03 x 2
GFDL-ESM4	r1i1p1f1	1 x 1.25
GISS-E2-1-G	r1i1p1f2	2 x 2.5
GISS-E2-1-H	r1i1p1f2	2 x 2.5
IPSL-CM6A-LR	r1i1p1f1	1.27 x 2.5
KACE-1-0-G	r1i1p1f1	1.25 x 1.88
MIROC-ES2L	r1i1p1f2	2.79 x 2.81
MIROC6	r1i1p1f1	1.4 x 1.41
MRI-ESM2-0	r1i1p1f1	1.12 x 1.12
NorESM2-LM	r1i1p1f1	1.89 x 2.5
NorESM2-MM	r1i1p1f1	0.94 x 1.25
TaiESM1	r1i1p1f1	0.94 x 1.25
UKESM1-0-LL	r1i1p1f2	1.25 x 1.88

Table S7: Estimated annual excess deaths due to wildfire smoke at the state level. For historical period, the table shows average annual excess deaths due to smoke $PM_{2.5}$ exposure during 2011-2020. For future climate scenarios, the table shows average annual excess deaths due to smoke $PM_{2.5}$ exposure during 2046-2055 (median across 28 GCMs).

State	Historical	SSP1-2.6	SSP2-4.5	SSP3-7.0	State	Historical	SSP1-2.6	SSP2-4.5	SSP3-7.0
California	1381	4164	4657	5700	South Carolina	266	327	353	380
Texas	1276	1974	1958	1999	Tennessee	360	283	358	373
Washington	360	1108	1266	1530	Massachusetts	283	257	330	359
Florida	821	1119	1198	1295	Montana	87	219	253	318
Oregon	411	858	1020	1245	Mississippi	184	295	302	306
New York	800	749	924	979	Arkansas	244	323	305	302
Michigan	610	807	819	825	Kentucky	256	238	285	291
Ohio	651	701	845	821	Iowa	243	277	283	286
Pennsylvania	633	617	759	820	Kansas	224	265	260	269
Illinois	779	746	862	817	Utah	92	186	245	259
North Carolina	442	575	612	667	Maryland	236	168	213	232
Georgia	447	567	606	643	New Mexico	82	175	188	212
Arizona	184	511	558	574	Connecticut	162	150	193	201
Nevada	117	421	463	560	Nebraska	147	168	167	180
Colorado	225	398	497	540	West Virginia	94	69	101	109
Virginia	288	431	467	497	Wyoming	31	72	81	99
Wisconsin	366	461	464	471	South Dakota	63	81	85	91
Missouri	476	406	453	462	Maine	62	59	79	87
Indiana	392	394	464	452	New Hampshire	54	59	74	79
Louisiana	274	440	438	441	North Dakota	53	63	67	77
New Jersey	394	328	406	437	Rhode Island	49	43	55	61
Idaho	100	296	348	431	Delaware	44	24	33	37
Minnesota	340	399	405	418	Vermont	26	25	32	35
Alabama	306	358	391	409	D.C.	29	25	32	33
Oklahoma	320	415	394	404					

Supplementary figures

A

Model	Evaluation	R	RMSE/mean	Bias
Our model	LOOCV	0.95	22%	-6%
log(fire) ~ VPD	LOOCV	0.34	42%	-44%
XGBOOST grid	LOOCV	0.48	82%	-1%
XGBOOST grid	Random CV	1.00	23%	6%

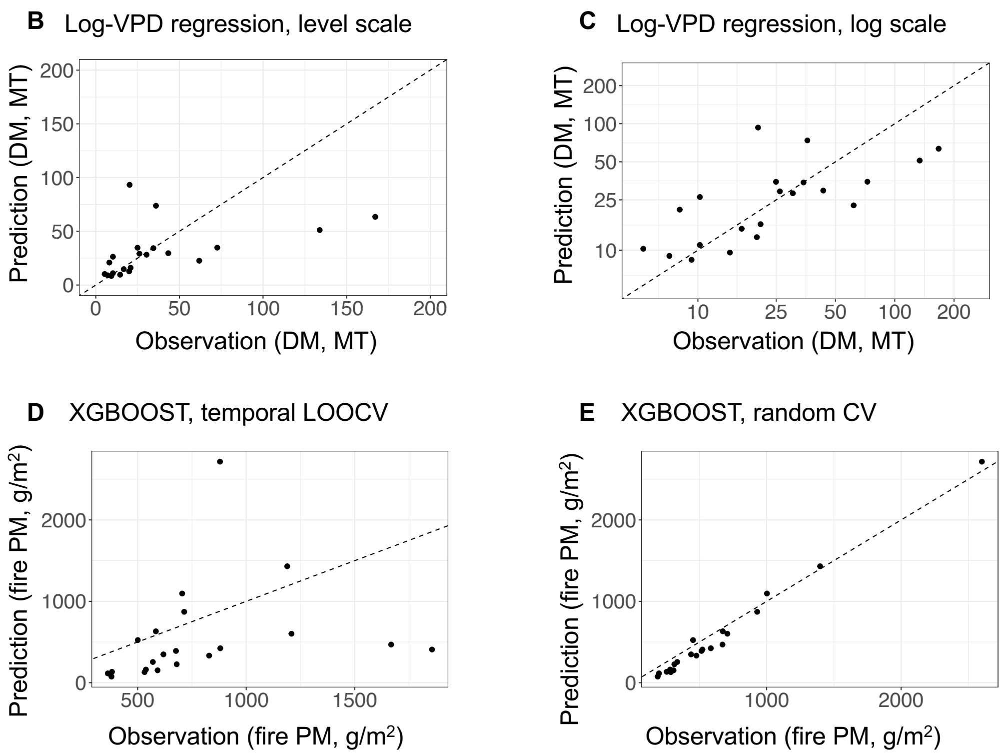

Figure S1: Predictive performance of our model and two other approaches used in previous research to predict wildfire emissions using climate variables. For comparison purposes, this figure only shows the results in western US. Panel A compares the predictive performance between our ensemble statistical and machine learning model ("Our model"), a regression method that uses fire-season VPD to predict the logged fire emissions ("log(fire)-VPD") as used in (*25*), and a XGBOOST model that predicts the fire emissions at the grid cell level as used in (*26*). The table shows the correlation coefficient (R), RMSE/mean, and bias of the highest-emitting 10-year period. Panels B and C show the out-of-sample prediction from the log(fire)-VPD regressions, with the same underlying data shown in level scale (B) and log scale (C). This demonstrates that while log(fire)-VPD regression achieves reasonable performance in the log scale (as reported by previous papers), its performance is inferior to our models in predicting the absolute levels of fire emissions. Panels D and E show the out-of-sample predictions from XGBOOST model under temporal LOOCV (D) and random CV (E) using the underlying dataset from (*26*). Random CV randomly partitions data to training and test sets with the same grid cell from different years possibly existing in both training and test sets. Panels D and E suggest the XGBOOST model trained at the grid cell has an inflated performance under random CV which grid cells can contribute data to both training and test sets.

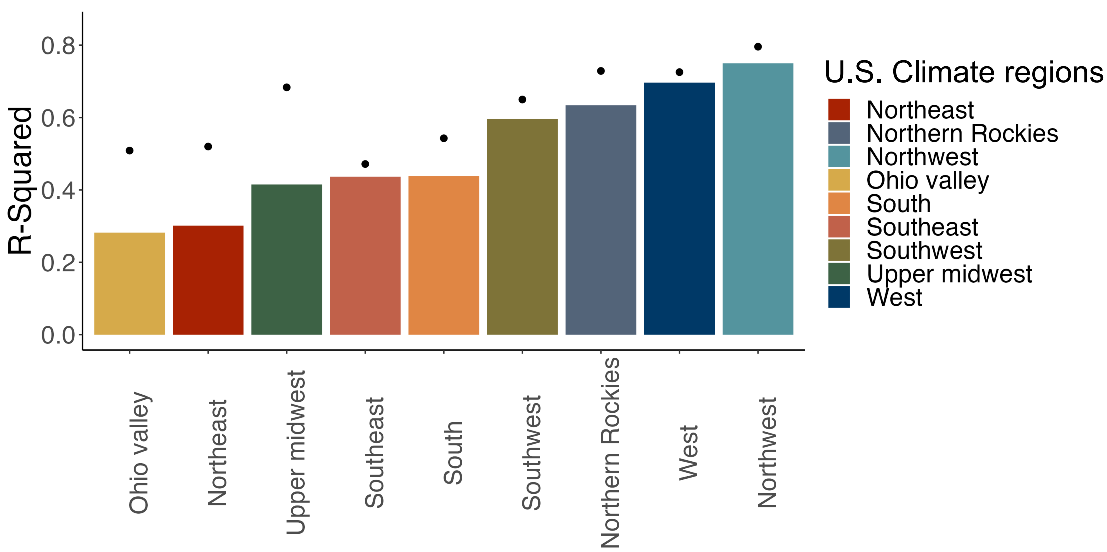

Figure S2: Performance of the fire-smoke regression models. The black dots show the full adjusted R^2 of the regression model. The color bars show the within R^2 after partialing out the month-of-year and grid cell fixed effects. The within R^2 thus quantify the model predictive performance within each grid cell and month-of-year. Each bar shows the performance of a fire-smoke model in one of the nine US climate regions.

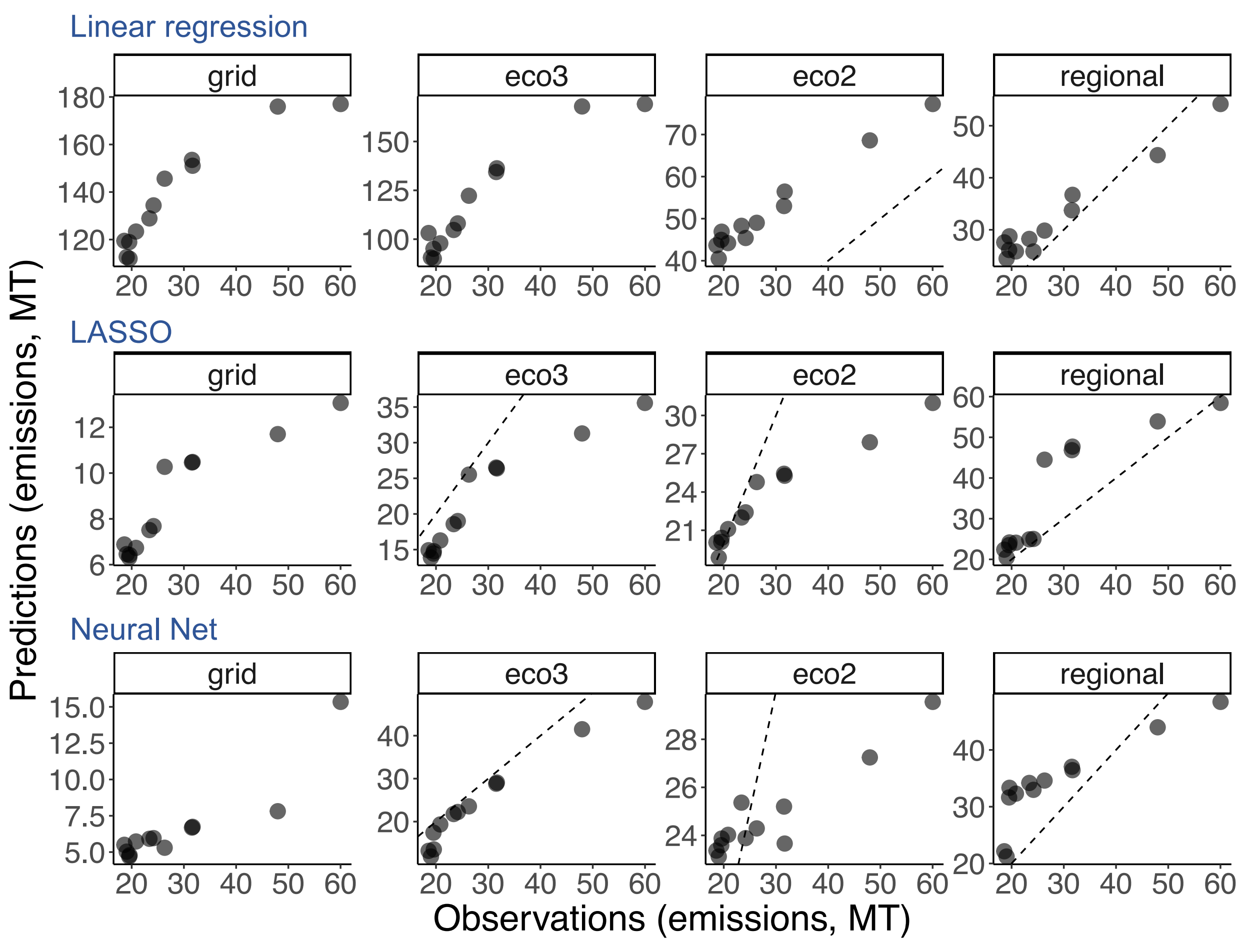

Figure S3: Predictive performance of models trained at different spatial resolutions (Western US). The plot shows the 10-year moving average of predicted emissions (y-axis) against the observed emissions (x-axis) from models trained at different spatial resolutions. For each algorithm (row), results are presented for models trained using grid cell data ("grid"), data aggregated at the level-3 ecoregion ("eco3"), data aggregated at the level-2 ecoregion ("eco2"), and data aggregated at the regional level ("regional"). Despite the different spatial resolutions of training data, the evaluation is at the regional level: we first aggregate the out-of-sample prediction to the regional level and compare the aggregated predictions against the aggregated observations. Dashed lines are 1-1 lines.

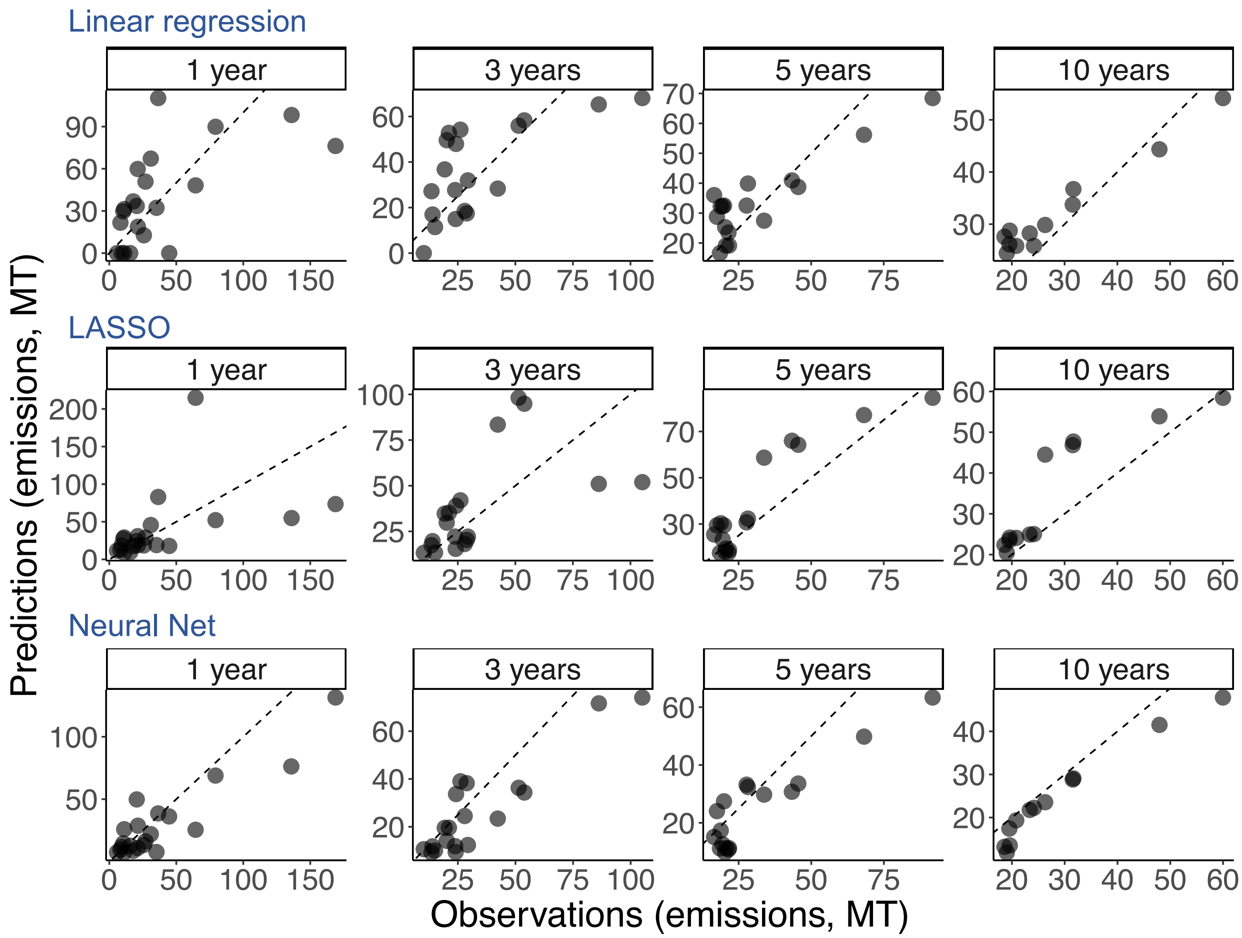

Figure S4: Predictive performance of models evaluated at different temporal scales (Western US). The plot shows the 10-year moving average of predicted emissions (y-axis) against the observed emissions (x-axis) from the same set of model but evaluated at different temporal scales. For each algorithm (row), the results show the out-of-sample prediction aggregated at different temporal scales ranging from no-aggregation (i.e. 1 year), to aggregation at the 10-year intervals. Dashed lines are 1-1 lines.

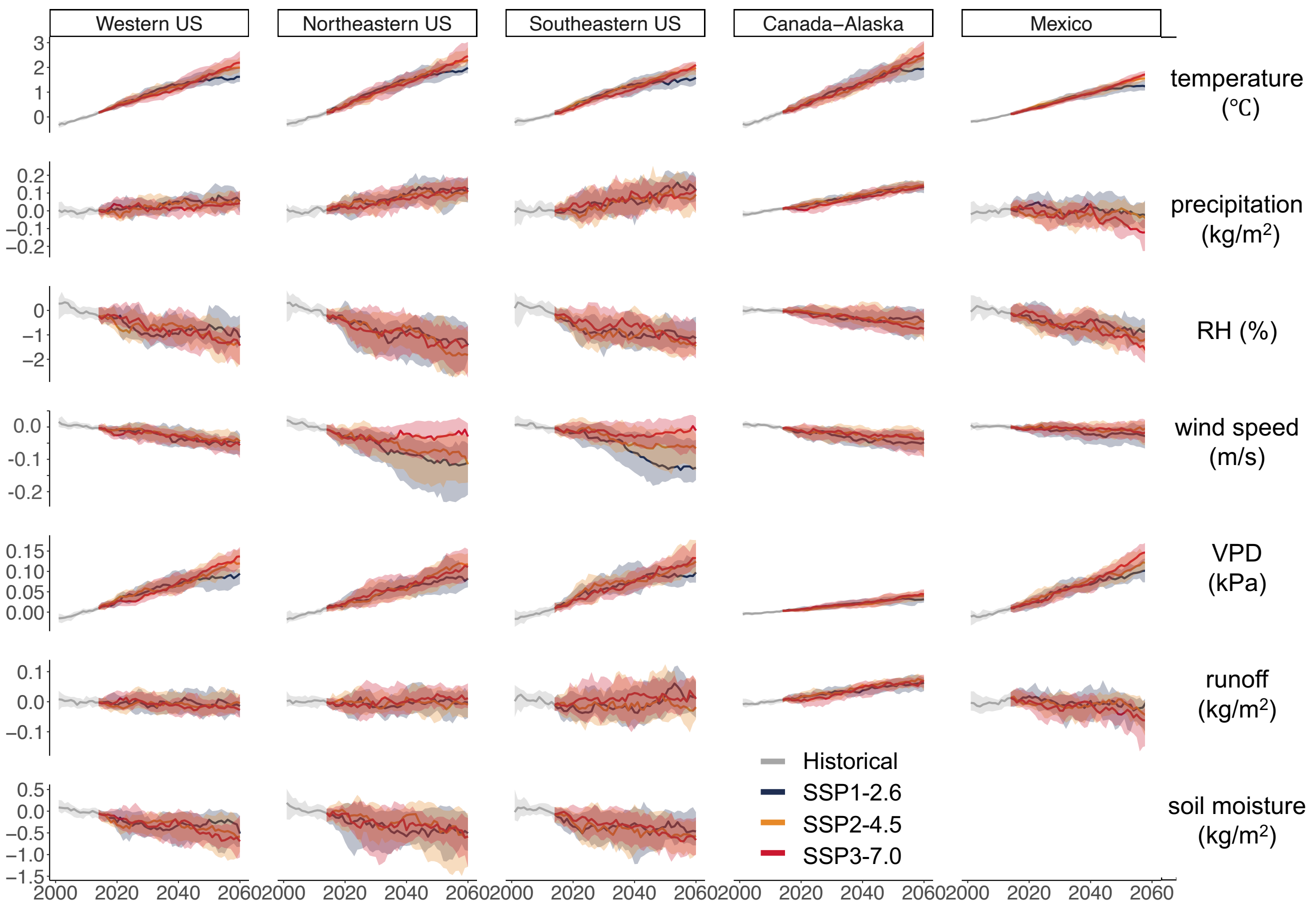

Figure S5: Projections of the climatic variables used in our statistical and machine learning models. Colour line indicates the median across 28 GCMs, and the shade area shows the 25th and 75th percentile across GCMs. The plot shows the 10-year moving average of the anomalies of each variable relative to the average values under historical scenario during 2001-2014. Soil moisture is not shown in Canada-Alaska and Mexico, as historical observations of soil moisture from NLDAS-2 are not available for these two regions.

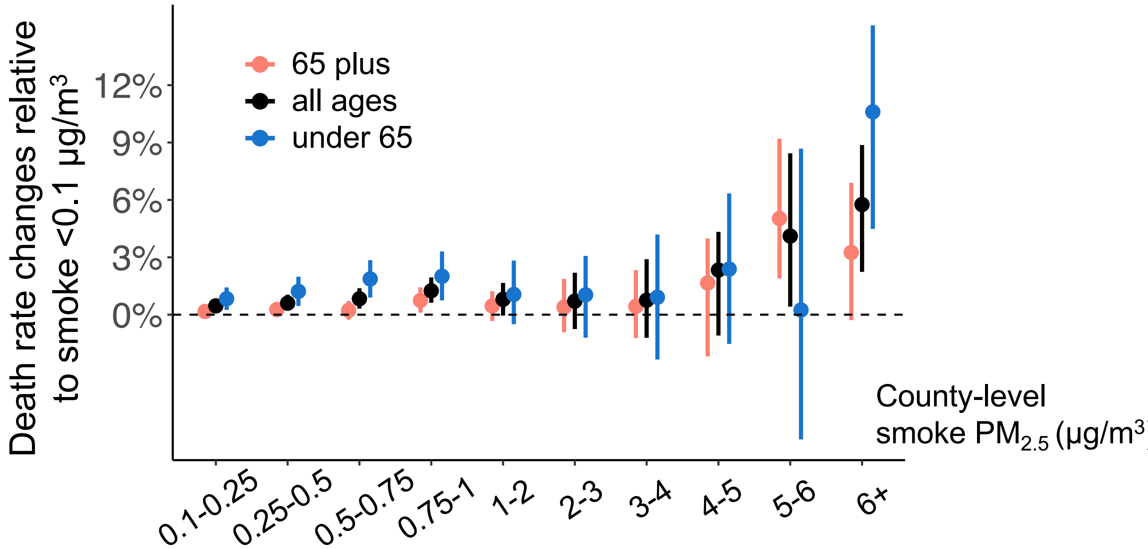

Figure S6: Impacts of smoke $PM_{2.5}$ concentration on mortality rates estimated by age group. The figure shows the effects of exposure to different annual mean concentration of smoke $PM_{2.5}$ (x-axis) relative to a no-smoke year (defined as a year with smoke $PM_{2.5}$ concentration less than 0.1 $\mu g/m^3$), estimated using a Poisson model at the county and annual level. The error bars show the 95% confidence interval estimated using bootstrap.

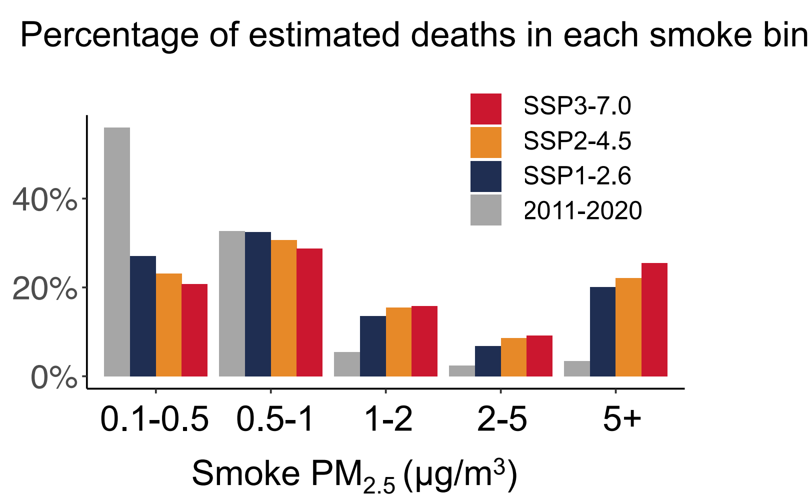

Figure S7: Percentage of estimated death contributions from each smoke concentration bin. The plot shows the contribution to total smoke-related deaths from county-years with annual mean smoke concentrations that fall in different smoke concentration bins under each scenario.

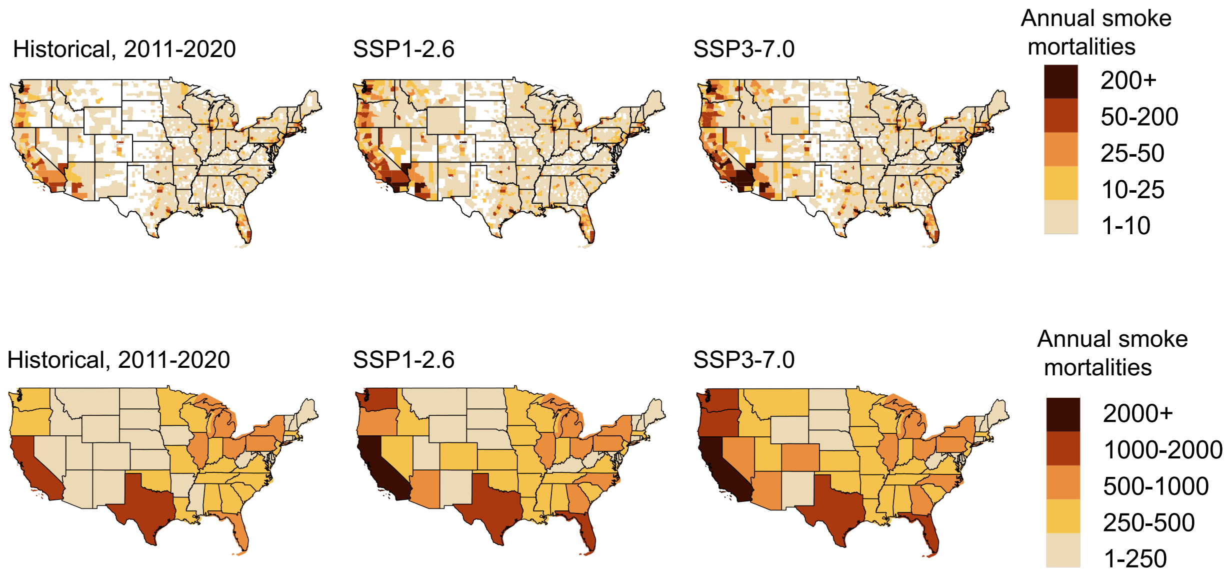

Figure S8: Estimated annual excess deaths due to smoke $PM_{2.5}$ under the historical, SSP1-2.6, and SSP3-7.0 scenarios. The top panels show estimates at the county level. The bottom panels show estimates at the state level.

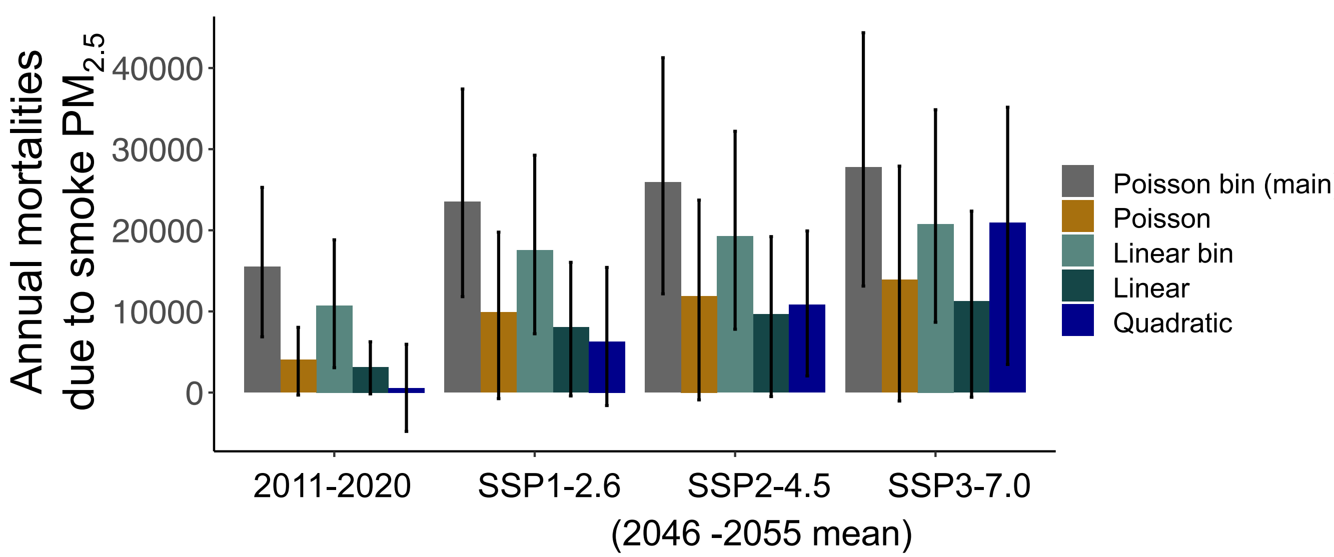

Figure S9: Estimated annual excess deaths due to smoke $PM_{2.5}$ across alternative dose-response functions. Our main analysis uses the "Poisson bin" specification. The error bars show the 95% confidence interval estimated using bootstrap.

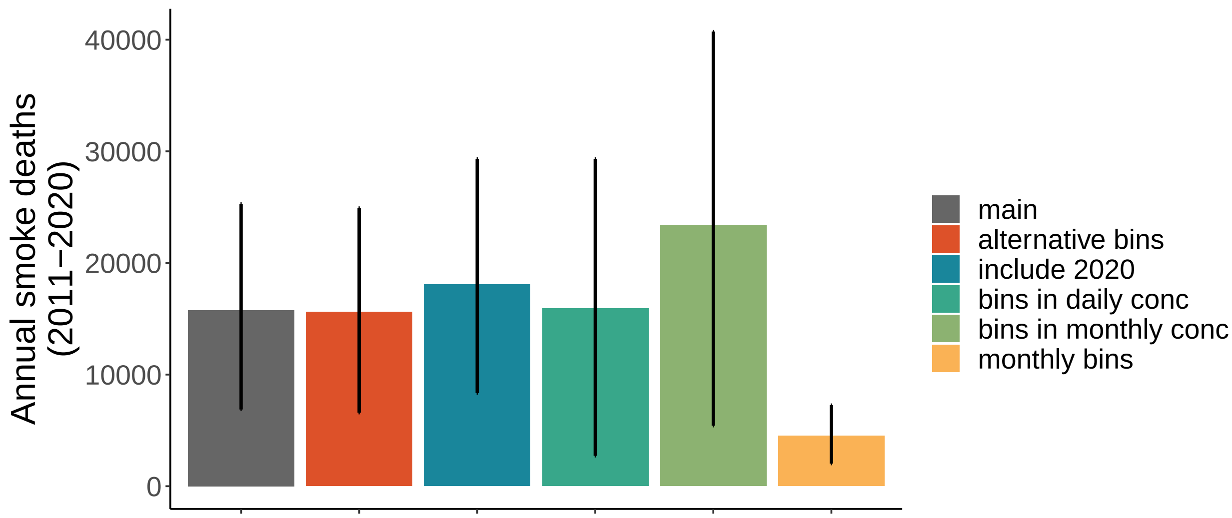

Figure S10: Estimated annual excess deaths due to smoke $PM_{2.5}$ (2011-2020) across alternative specifications of the Poisson model. In addition to our main model (grey bar), we estimate a model which uses alternative bin definitions, a model which includes year 2020, a model which calculates the number of months or the number of days in a year that fall in different smoke bins to represent different temporal aggregations, and a model which is estimated at the county-month level. The error bars show the 95% confidence interval estimated using bootstrap.

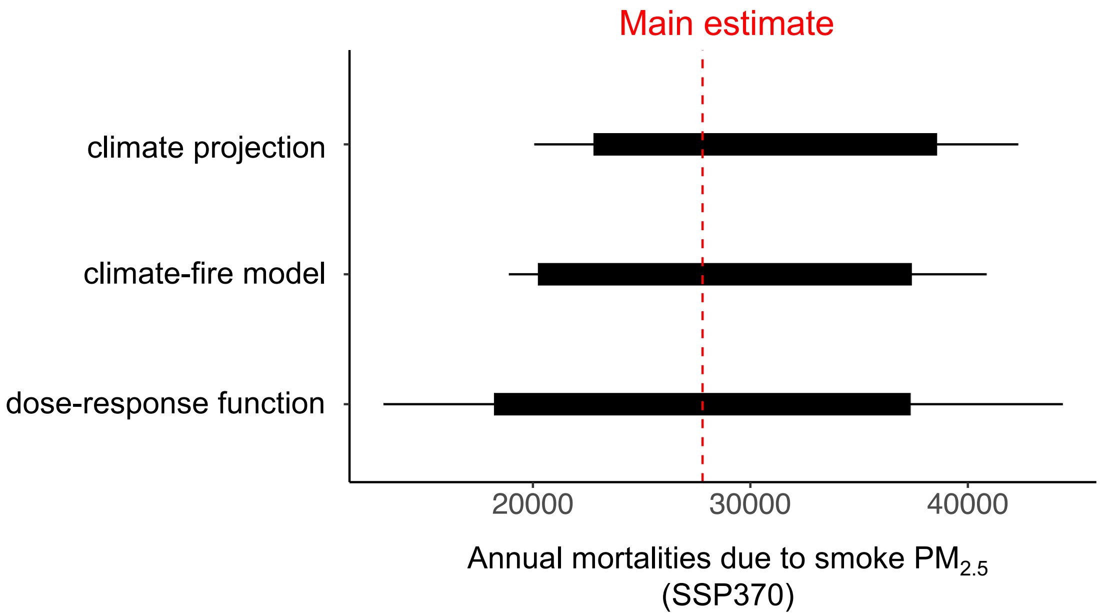

Figure S11: Uncertainty in estimated annual excess deaths due to wildfire smoke $PM_{2.5}$ under SSP3-7.0 scenario. The figure shows the uncertainty of the mortality estimates due to climate projections, climate-fire model, and the dose-response function between smoke and mortality. The red dashed line shows the main estimate reported in the paper (i.e. 27,800 excess deaths per year). The solid bar shows the 10th and 90th percentile, and the black line shows the 2.5th and 97.5th percentile. Uncertainty from "climate projection" is calculated using the percentiles of the estimated mortality from the 28 GCMs. Uncertainty from "climate-fire model" is calculated using bootstrap procedures performed on the individual fire-climate models from each region. More specifically, we first construct bootstrapped samples of the fire-climate panel dataset (sample with replacement) and then fit fire-climate model from each bootstrapped sample, and use these models to project smoke deaths. Uncertainty from "dose-response function" is calculated using bootstrap procedures performed on the health response functions. More specifically, we construct bootstrapped samples of the smoke-death dataset and estimate one dose-response function from each sample.

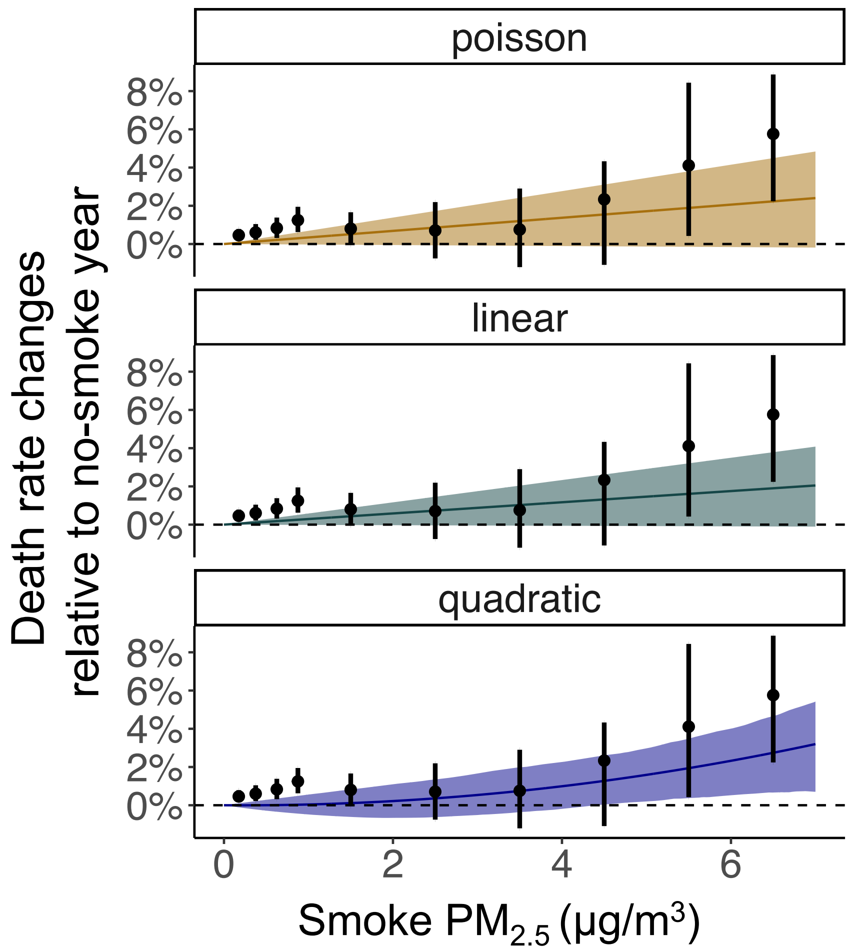

Figure S12: Impacts of smoke $PM_{2.5}$ concentration on mortality rates estimated using three alternative dose-response functions. The three colour lines show the estimated results from three non-binned models with poisson, linear, and quadratic specifications. For comparison, the black dots show the estimated coefficients from our main model (Poisson bin model). The shaded areas and the error bars represent the 95% confidence interval estimated using bootstrap procedure.